

Inelastic electron transport in granular arrays

Alexander Altland¹, Leonid I. Glazman^{2,3}, Alex Kamenev², and Julia S. Meyer⁴

¹*Institut für Theoretische Physik, Universität zu Köln, 50937 Köln, Germany*

²*Department of Physics, and ³W.I. Fine Theoretical Physics Institute, University of Minnesota, Minneapolis, MN55455, USA*

⁴*Materials Science Division, Argonne National Laboratory, Argonne, IL60439, USA, and Department of Physics, The Ohio State University, Columbus, OH43210, USA*

(Dated: September 1, 2018)

Transport properties of granular systems are governed by Coulomb blockade effects caused by the discreteness of the electron charge. We show that, in the limit of vanishing mean level spacing on the grains, the low-temperature behavior of 1d and 2d arrays is insulating at any inter-grain coupling (characterized by a dimensionless conductance g). In 2d and $g \gg 1$, there is a sharp Berezinskii-Kosterlitz-Thouless crossover to the conducting phase at a certain temperature, T_{BKT} . These results are obtained by applying an instanton analysis to map the conventional ‘phase’ description of granular arrays onto the dual ‘charge’ representation.

PACS numbers: 73.23.-b, 73.23.Hk, 71.45.Lr, 71.30.+h

I. INTRODUCTION

It has been long appreciated that the low-temperature physics of generic disordered metals is characterized by a subtle interplay of electron-electron interactions and coherent disorder scattering. While both effects are of crucial importance, their unified treatment still evades a complete theoretical description. It is useful, thus, to approach them separately. The limiting case of “coherence without interactions” has been studied intensely. It is well understood that the coherent multiple scattering off impurities leads to Anderson localization: in one and two dimensions all states are localized¹. While in homogeneously disordered systems this phenomenon has always to be taken into account, granular systems admit for a parameter regime where the physics is entirely controlled by interaction effects. It is the purpose of this paper to explore the regime of “interactions without coherence” accessible in metallic granular arrays.

Metallic granular arrays are also of great interest in their own right^{2,3,4,5,6,7,8,9,10,11,12,13,14,15}. In particular, strongly coupled arrays ($g \gg 1$, where g is the dimensionless inter-grain conductance) have become a subject of increased theoretical attention in recent years^{8,9,10,11,12,13,14}. An isolated grain or quantum dot is characterized by three energy scales: the Thouless energy E_{Th} , the charging energy E_c , and the mean level spacing δ . The tunneling coupling between the grains adds another parameter: the dimensionless conductance g of a contact between two neighboring grains. Throughout this paper we focus on the regime, where the Thouless energy E_{Th} is the largest energy scale. This allows one to treat each grain as a zero-dimensional object and disregard the intra-grain in comparison with the inter-grain resistance. The interaction effects are controlled by the charging energy E_c (in the simplest model $E_c = e^2/(2C)$, where C is the self-capacitance of a grain.) In our studies it is the next largest energy scale in the system. Finally, quantum coherence effects are governed by the energy

scale(s) $\propto \delta$. If such a scale is much smaller than all relevant temperatures, one may treat each grain as having a *continuous* spectrum. This assumption allows one to disregard phase coherence. In essence: an electron exiting a grain is never the same electron that has previously entered it.

The parameter regime specified above justifies the “interactions without coherence” program. It is clear though, that such a simplification cannot work down to the very smallest temperatures. At low enough temperature, coherent propagation through multiple grains will become important and our approximation is bound to fail. It is, thus, important to realize that the subject of our considerations is a transient (though possibly wide) temperature range. In this range, coherence may be disregarded while interactions (and inter-grain tunneling) are crucially important in determining the electrical properties of the array.

At small inter-grain conductance $g \ll 1$, an electron is completely localized within a single grain. Therefore, the problem is reduced to the description of *classical* charges moving on the lattice (which is a simple limiting case of the considerations given below.) In the simplest case of on-site interactions only, there is an energy barrier E_c impeding the transition of electrons between two neighboring grains. It is thus natural to expect activation behavior of the conductivity, with the activation temperature $T^* = E_c$.

The present paper is devoted to the more intricate case of large inter-grain conductances, $g \gg 1$. In this case the charge may spread over many grains to decrease its charging energy. The interplay of interactions and tunneling dictates that this spreading involves an (exponentially) large, but *finite* number of grains. As a result, the lowest energy excitations of the system are large single-charge *solitons*. The activation energy for creating such an extended charge carrier is substantially reduced, leading to

the low-temperature conductivity of the form:

$$\sigma(T) = g \exp \left[-\frac{T^*}{T} \right], \quad (1)$$

where $T_{(1d)}^* \sim gE_c \exp[-g/4]$ and $T_{(2d)}^* \sim g^2 E_c \exp[-g]$. The important consequence of Eq. (1) is that one- and two-dimensional arrays are insulating at arbitrarily large inter-grain conductance, g . This is a pure interaction effect; Anderson localization physics is *not* included in the model. Switching off the interactions, one obtains Ohmic metallic behavior with a temperature-independent conductivity.

The solitons interact with each other up to distances comparable to their (exponentially large) radius, even if the initial model possesses on-site interactions only. Once they start to overlap, Eq. (1) is not valid anymore. In 1d this happens at $T \sim T_{(1d)}^*$, where the conductivity smoothly crosses over to its high-temperature behavior⁹ $\sigma_{(1d)}(T) = g - 2 \ln(gE_c/T)$. In two dimensions, the solitons interact logarithmically over a large range of distances. This leads to a Berezinskii-Kosterlitz-Thouless (BKT) unbinding of soliton-anti-soliton pairs^{16,17} at the temperature

$$T_{\text{BKT}} = T_{(2d)}^*/g \ll T_{(2d)}^*. \quad (2)$$

Around this temperature the conductivity undergoes a sharp crossover from the exponentially small value given by $\sigma(T_{\text{BKT}})$, cf. Eq. (1), up to the high-temperature asymptotics, $\sigma_{(2d)}(T) = g - \ln(gE_c/T)$. In the model with only mutual capacitances between neighboring grains the Coulomb interaction is logarithmic at arbitrarily large distances. This results in a true BKT phase transition with zero conductivity below the transition point. The $g \ll 1$ version of the latter model was previously considered in Refs. [3,18]. The introduction of on-grain Coulomb interactions transforms the transition into a crossover. Interestingly, for $g \gg 1$ the BKT remains sharp even for the pure on-grain (self-capacitance only) Coulomb interactions.

Technically we approach the problem from two complementary perspectives: the *phase* and the *charge* representations. The former is straightforwardly derived from the microscopic fermionic model¹⁹. It is commonly employed in the study of both homogenous and granular interacting systems. While being effective in the high-temperature regime, it becomes increasingly difficult to handle at lower temperatures. To treat this latter regime, we employ the charge model, introduced previously within the context of quantum dot physics^{20,21}. Our main technical achievement is the proof of equivalence of these two approaches over a parametrically wide range of temperatures. For these temperatures, both models may be handled in a *controlled* way. We thus conclude that the charge model, although not directly deduced from the microscopic Hamiltonian, is indeed the proper description of the low-temperature phase of the system. The results mentioned above (as well as others

discussed below) then follow in an almost straightforward manner from the charge description.

The equivalence of the two approaches is based on a very important observation. The charge discreteness (crucial in the low-temperature insulating phase) manifests itself in the phase model through the 2π -periodicity of the phase field (the internal space of the field is the circle S^1 .) The latter results in the existence of topologically distinct stationary-point field configurations, classified by the integer winding numbers $W_{\mathbf{l}}$ (where the vector index \mathbf{l} numerates the grains on the lattice.) In strongly connected arrays, $g \gg 1$, the action cost for configurations with non-zero winding numbers (so-called Korshunov instantons²²) is exponentially large. However, one has to take into account Gaussian fluctuations around the topologically non-trivial stationary points, which yield a factor $(gE_c/T)^{1/d}$ for each winding number mismatch between neighboring grains. This factor suggests that the instanton configurations are increasingly important at low temperatures²³. Summation of the instanton “gas” along with the corresponding Gaussian fluctuations and the phase-volume factors results exactly in the classical (low-frequency) limit of the d -dimensional charge model. Specifically (see below), the instanton expansion of the phase model coincides term by term with the perturbative expansion in back-scattering amplitudes of the charge model. Therefore, we are convinced that the explicit account for instantons in the phase-like models is imperative to restore the charge discreteness and, thus, to describe the insulating phase.

One may justifiably worry about the role of non-Gaussian fluctuations. The latter are known to become large at a low enough temperature $T_0 \sim E_c e^{-dg/2}$, violating the validity of the instanton gas picture. Crucially, however, (in 1d and 2d) the corresponding charge model predicts an activation gap which is *parametrically larger* (exponential (in g) in 1d and algebraic in 2d) than T_0 . As a result, there is a wide range of temperatures, where the fluctuations are well under control, while the physics is completely dominated by the proliferation of instantons. The latter results in the appearance of the unit-charge extended solitons as low-energy charged excitations and, thus, in activation insulating behavior, Eq. (1). In 3d, proliferation of instantons and the onset of strong non-Gaussian fluctuations, resp., take place at comparable temperatures. As a result the phase-charge equivalence cannot be reliably established. It seems plausible, however, that the instanton gas — and thus the corresponding charge representation — provide a qualitatively correct description of the 3d insulator as well.

This paper is an extension of two previous shorter publications [10,11]. Its intent is two-fold. Firstly, we present some new results. In particular, we extend calculations beyond the tunneling limit, accounting for arbitrary transmission amplitudes between neighboring grains. Furthermore, in addition to an evaluation of the transport properties, we discuss the behavior of the single-particle density of states (DoS). Secondly, we bring

out the philosophy of our approach and expose extensive technical details of the calculations. Our main message is that charge quantization is crucial in describing the low-temperature physics of the array — and, therefore, a description in terms of charge degrees of freedom is appropriate. As mentioned above, this description is obtained by accounting for topologically non-trivial field configurations in the phase picture. This goes beyond the commonly used perturbative treatment of the phase model. In 1d and 2d arrays, the latter completely misses the appearance of a new temperature scale T^* marking the crossover to insulating behavior.

The paper is organized as follows: in Sec. II, we introduce the phase and charge models. Before coming to the main part, namely quantum dot arrays, in Sec. III, we discuss the physics of a single dot connected to two leads. Sec. IV discusses one-dimensional arrays whereas Sec. V contains the two-dimensional arrays. The conclusion and open questions are discussed in Sec. VI.

II. PHASE AND CHARGE REPRESENTATIONS

In this section, we introduce two effective models used to describe d -dimensional quantum dot arrays. As mentioned in the introduction, the two descriptions are optimally adjusted to the nominally metallic and the nearly insulating regime, respectively. The application of the two models to the computation of observables, and the mapping of one onto the other will be discussed in later sections.

Widely used in the literature is the so-called Ambegoakar-Eckern-Schön (AES) model^{6,19} — a description of arrays in terms of phase fields. In the limit of vanishing level spacing, this model may be derived starting from a microscopic description in terms of electronic degrees of freedom. The model is presented in Sec. II A, and its derivation is reviewed in App. A 1.

While the AES approach provides an efficient description of the high-temperature regime, it is untractable in the low-temperature regime where interaction effects become significant. Rather, at low temperatures, an alternative description in terms of charge degrees of freedom is more appropriate. This latter formulation may be derived from a phenomenological model introduced by Flensberg²⁰ and Matveev²¹. We review the derivation in Sec. II B.

The equivalence of the two models — established by a mapping between them — will be discussed at later stages.

A. Phase model

In the regime, where the level spacing of the dot is negligible, the dot can be described by a single degree of freedom. Starting from a description in terms of electrons, a phase field ϕ is introduced to decouple the inter-

action on the dot. Subsequently the electronic degrees of freedom can be integrated out, yielding an effective theory in terms of ϕ . The time-derivative of ϕ corresponds to the voltage V on the dot: $V(\tau) = \dot{\phi}(\tau)$, where τ is imaginary time.

Since the AES model is largely standard by now, we here restrict ourselves to a brief discussion of its main elements. (For an outline of its derivation, see App. A 1.) The phase action S consists of two terms, $S = S_c + S_t$, describing the charging interaction on the grains and the tunneling between neighboring grains, respectively. For the d -dimensional array geometry, the charging term reads

$$S_c[\phi] = \sum_{\mathbf{l}} \int d\tau \left(\frac{\dot{\phi}_{\mathbf{l}}^2}{4E_c} - iq\dot{\phi}_{\mathbf{l}} \right), \quad (3)$$

where \mathbf{l} is a d -dimensional index, denoting the position of the grain. Here, $E_c = e^2/(2C)$ is the charging energy, where e is the electronic charge and C the self-capacitance of the dot. The dimensionless quantity $q = V_g C/e$ is the background charge on the dot as determined by an external gate voltage V_g . The phase fields $\phi_{\mathbf{l}}$ obey the boundary condition $\phi_{\mathbf{l}}(\beta) - \phi_{\mathbf{l}}(0) = 2\pi W$ (where $W \in \mathbb{Z}$).

The tunneling term is given by:

$$S_t[\phi] = -\frac{1}{16} \sum_{(\mathbf{l}, \mathbf{l}')} \sum_k \kappa_k \text{tr} \left[(\Lambda e^{i\phi_{\mathbf{l}'}} \Lambda e^{-i\phi_{\mathbf{l}}})^k \right], \quad (4)$$

where $\phi_{\mathbf{l}'} = \phi_{\mathbf{l}} - \phi_{\mathbf{l}'}$. The matrix Λ takes the form $\Lambda_{nm} = \delta_{nm} \text{sign}(\epsilon_n)$ in Matsubara basis ($\epsilon_n = 2\pi(n + 1/2)T$). Furthermore, the coefficients κ_k are related to the tunneling matrix elements T_α and the density of states ν as $\kappa_k = -4 \frac{(-1)^k}{k} \sum_\alpha |\pi \nu T_\alpha|^2 k$. (Note that we do not need to require the transmission in every channel, α , to be small — tunneling can be taken into account to arbitrary order²⁴.)

Having presented an effective action for the phase field ϕ , we proceed by discussing its properties. A large inter-grain conductance g suppresses dynamical phase fluctuations: in a conductor, voltage fluctuations are small. As a first step, one may, thus, expand the action up to second order in ϕ . The quadratic tunneling action reads

$$S_t^{(2)}[\phi] = \frac{gT}{4\pi} \sum_{(\mathbf{l}, \mathbf{l}')} |\omega_m| \phi_{\mathbf{l}', m}^2. \quad (5)$$

Here, the dimensionless conductance of the contacts, g , is given by²⁴

$$g = \sum_k k^2 \kappa_k = \sum_\alpha \mathcal{T}_\alpha, \quad (6)$$

where $\mathcal{T}_\alpha = 4\pi^2 \nu^2 |T_\alpha|^2 / (1 + \pi^2 \nu^2 |T_\alpha|^2)^2$ is the transmission probability in the channel α . The action (5) describes Ohmic dissipation. Evaluating transport properties of the array within this approximation, one obtains the classical Kirchhoff laws.

Going beyond the quadratic approximation⁹, however, one finds that the conductance is renormalized to smaller values upon lowering the temperature. Taking into account the terms quartic in ϕ , one obtains the renormalized inter-grain conductance,²⁵

$$g \rightarrow g - \frac{2}{dg} \sum_{\alpha} \mathcal{T}_{\alpha} (1 - \mathcal{T}_{\alpha}) \ln \frac{gE_c}{T}. \quad (7)$$

In the tunneling limit ($\mathcal{T}_{\alpha} \ll 1$), Eq. (7) reduces to⁹ $g(T) = g - (2/d) \ln(gE_c/T)$.

Eq. (7) states that in all dimensions interactions generate logarithmic corrections to the inter-grain conductance g . This result holds as long as the corrections are small. Perturbation theory breaks down at the temperature where the corrections become of order of the bare conductance or, in other words, the renormalized conductance $g(T)$ reaches values of order 1. This defines a temperature scale $T_0 \sim E_c e^{-dg/2}$. The temperature range below this scale is beyond the applicability of the perturbative treatment.

However, there is more to be extracted from the AES model even at $T \gg T_0$. Let us return to the full action Eqs. (3) and (4). The phase field ϕ_1 is a periodic variable $\phi_1(\beta) - \phi_1(0) = 2\pi W$. Consequently, the conjugate variable — which is charge — is quantized. By using the perturbative expansion in ϕ_1 around the minimum $\phi_1 = 0$, all information about periodicity and, therefore, about charge quantization is lost. Although for $g \gg 1$ phase fluctuations are heavily suppressed, there are ϕ_1 -configurations that explore this periodicity and, thus, incorporate the manifestations of charge quantization. As we show in this paper, these phase *instantons*²² provide the key to access the insulating phase of arrays.

Before discussing the instanton physics in single quantum dots as well as one- and two-dimensional arrays, we introduce the aforementioned alternative model to describe the system.

B. Charge model

In this section, we introduce a phenomenological model describing the system in terms of charge degrees of freedom, i.e., those degrees of freedom that become approximately conserved in near insulating regimes and, therefore, are optimally suited to describe the low-temperature physics of the system.

Let us start by considering a point contact between a quantum dot and a metallic reservoir. Due to size quantization effects, no more than a few transverse modes $\alpha = 1, \dots, N$ are permitted to transport charge across the contact. Each of these modes may be thought of as a one-dimensional electron liquid. For simplicity, we focus on the case of just one propagating mode $N = 1$ throughout. The generalization to multi-mode contacts — essential in order to describe the case of large dimensionless inter-grain conductance $g \gg 1$ — is discussed in appendix B 1.

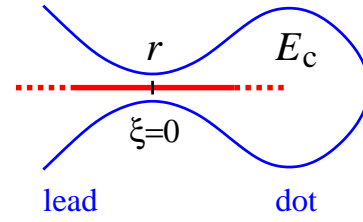


FIG. 1: (Color online) Schematic representation of the charge model. The line in the middle indicates a clean (infinite) 1d channel with a single impurity, having backscattering amplitude r .

Bosonizing the one-dimensional electron liquid in the conventional way^{20,21}, the system is described in terms of a bosonic field $\theta(\tau, \xi)$. The gradient of this field, $\partial_{\xi}\theta(\tau, \xi)$, defines the local electron density, i.e., the electron number on the dot may be written as $\mathcal{N} = \int_0^{\infty} d\xi \partial_{\xi}\theta(\tau, \xi) = -\theta(\tau, 0)$. This implies that the Coulomb energy takes the simple form $(e\mathcal{N})^2/(2C) = E_c\theta^2(\tau, 0)$. Finally, accounting for backscattering by introducing a point scatterer of reflection amplitude r at coordinate $\xi = 0$ (cf. Fig. 1), the imaginary-time action of the bosonic field reads

$$S[\theta(\tau, z)] = \int_0^{\beta} d\tau \left\{ \int_{-\infty}^{\infty} d\xi [(\partial_{\tau}\theta)^2 + (\partial_{\xi}\theta)^2] + E_c\theta^2(\tau, 0) - \frac{Dr}{\pi} \cos[2\pi\theta(\tau, 0)] \right\}, \quad (8)$$

where D is the electronic bandwidth. Integrating over the fields $\theta(\xi \neq 0)$ — which is possible because their action is quadratic — we obtain

$$S[\theta] = \frac{1}{T} \sum_m (\pi|\omega_m| + E_c) \theta_m^2 - \frac{Dr}{\pi} \int_0^{\beta} d\tau \cos(2\pi\theta(\tau)) \quad (9)$$

as the effective action of a single remaining degree of freedom $\theta(\tau) \equiv \theta(\tau, 0)$. Here we have introduced the Matsubara representation $\theta_m = \int_0^{\beta} d\tau \theta(\tau) e^{-i\omega_m\tau}$, where $\omega_m = 2\pi Tm$. The dissipative term, $\pi|\omega_m|\theta_m^2$, appears as a consequence of the assumption that the mean level spacing is the smallest energy scale in the model, $\delta \rightarrow 0$. It is generated by integrating out the continuum spectrum of the degrees of freedom on the dot.

The above expression Eq. (9) can be easily generalized to the array geometry. A field $\theta_{i,1}$ is assigned to each contact, where the d -component index \mathbf{l} denotes its position within the array and $i = 1 \dots d$ labels its direction. In this notation, the instantaneous electron density on the grain \mathbf{l} is given by the lattice divergence, $\mathcal{N}_{\mathbf{l}} = \sum_i (\theta_{i,1+\mathbf{e}_i} - \theta_{i,1}) = \nabla \cdot \vec{\theta}_{\mathbf{l}}$ (where \mathbf{e}_i is a unit vector in i -direction and the vector notation $\vec{\theta}_{\mathbf{l}}$ is introduced.) The generalization of Eq. (9) reads:

$$S[\vec{\theta}_1] = \sum_1 \left\{ \frac{1}{T} \sum_m \left(\pi |\omega_m| \vec{\theta}_{1,m}^2 + E_c (\nabla \cdot \vec{\theta}_{1,m} - q \delta_{m,0})^2 \right) - \frac{Dr}{\pi} \sum_i \int_0^\beta d\tau \cos(2\pi \theta_{i,1}(\tau)) \right\}, \quad (10)$$

where D is again the bandwidth. As in the single dot expression Eq. (9), the first term in the action (10) describes the dissipative dynamics originating from integrating out degrees of freedom within the grains, the second term is responsible for the interaction effects, i.e., charging, and the third one describes backscattering in the contacts. Furthermore, we introduced the external gate voltage, q , as an additional control parameter.

As shown in appendix B 1, generalization to the N -channel case amounts to replacing the single reflection coefficient r by the product $\prod_{\alpha=1}^N r_\alpha$, where r_α is the reflection coefficient in channel α . We define the dimensionless parameter \mathcal{G}_0 as

$$\mathcal{G}_0 = - \sum_\alpha \ln |r_\alpha|^2 \Leftrightarrow \prod_\alpha r_\alpha = e^{-\mathcal{G}_0/2}. \quad (11)$$

Although the single channel expression Eq. (10) was obtained for a small reflection coefficient $r \ll 1$, its multi-channel generalization remains valid as long as $\mathcal{G}_0 \gg 1$ (i.e., individual reflection coefficients r_α may be arbitrary, $0 < r_\alpha < 1$.) For a tunneling contact $\mathcal{T}_\alpha \ll 1$, where $\mathcal{T}_\alpha = 1 - |r_\alpha|^2$ is the transmission coefficient in channel α , this product can be expressed through the dimensionless conductance $g = \sum_\alpha \mathcal{T}_\alpha$ within exponential accuracy as

$$\prod_\alpha r_\alpha = \exp \left[\sum_\alpha \ln \sqrt{1 - \mathcal{T}_\alpha} \right] \simeq \exp \left[-\frac{1}{2} \sum_\alpha \mathcal{T}_\alpha \right] = e^{-\frac{g}{2}}.$$

In this regime, the dimensionless parameter, $\mathcal{G}_0 \simeq g$.

The action (10) will be our starting point for exploring interaction effects in single dots as well as in arrays. We will use it as an alternative to Eqs. (3) and (4) and discuss the connections between the two descriptions in the following sections.

III. SINGLE QUANTUM DOT

The simplest setup on which the impact of interactions on transport through an almost open system can be studied is a single quantum dot coupled to two leads^{21,26}. Interesting in its own right, the discussion of the quantum dot will facilitate the development of the formalism required to describe arrays. We follow a three-step program: in Sec. III A the AES phase model is investigated, in Sec. III B the alternative charge description is used, and in Sec. III C the two procedures are compared.

A. Phase model

Consider a single quantum dot coupled to a left (L) and right (R) lead. In the limit of a vanishing level spacing $\delta \rightarrow 0$, the system may be described by the phase action Eqs. (3) and (4),

$$S = \int d\tau \left(\frac{\dot{\phi}^2}{4E_c} - iq\dot{\phi} \right) + \frac{1}{4} \sum_k \kappa_k \text{tr} \left[(\Lambda e^{i\phi} \Lambda e^{-i\phi})^k \right]. \quad (12)$$

The perturbative results one may derive from this action have been discussed in the previous section. Going beyond this level, we here include topologically non-trivial excitations and discuss the resulting charge quantization effects.

In addition to the constant solution $\phi = 0$, the tunneling part of the action is stationary on the so-called Korshunov instanton configurations²². These additional saddle point solutions are characterized by their winding number $W = (\phi(\beta) - \phi(0))/(2\pi)$ and can be represented as^{22,27,28,29}

$$e^{i\phi_W(\{z\}, \tau)} = \prod_{a=1}^{|W|} \left[\frac{e^{2\pi i \tau T} - z_a}{1 - \bar{z}_a e^{2\pi i \tau T}} \right]^{\text{sign } W}. \quad (13)$$

Here the $|W|$ complex parameters $z = (z_1 \dots z_{|W|})$ are subject to the condition $|z_a| < 1$. The temporal variation of ϕ corresponds to a voltage pulse $V = i\dot{\phi}$ on the dot: the parameters $1 - |z|$ determine the duration of the voltage pulse and $\arg z$ its instance ($z = 0$ corresponds to a linear phase profile or a constant voltage.)

In the limit $T \ll E_c$, the action is dominated by the tunneling term, implying that the Korshunov instantons are approximate saddle point configurations of the total action. Substituting Eq. (13) into the action (12), one finds that²⁹

$$S[\phi_W(\{z\})] \approx \mathcal{G}_0 |W| - 2\pi i W q, \quad (14)$$

where the dimensionless conductance \mathcal{G}_0 is given by (cf. Eq. (11)) $\mathcal{G}_0 = \sum_k \kappa_{2k-1}$. Apart from a small charging contribution, $S_c[\phi_W(\{z\})] = \pi^2 (T/E_c) \sum_{a,a'} (1 - |z_a|^2 |z_{a'}|^2) / ((1 - z_a z_{a'}^*)(1 - z_a^* z_{a'}))$, the action is independent of z_a , i.e., the variables z_a are instanton zero modes.

Due to the largeness of the parameter $\mathcal{G}_0 \gg 1$, the contribution of a single instanton is exponentially small. However, as will be shown in the following, fluctuations around the instanton trajectory increase with decreasing temperature²⁸, i.e., a temperature scale exists below which the instanton contributions become important.

The partition function Z can be represented as a sum over different winding number sectors:

$$Z = Z_0 \sum_W \frac{Z_W}{Z_0} e^{2\pi i W q}, \quad (15)$$

where Z_W is the contribution from configurations with winding number W . Note that a given total winding number W can be obtained by superposition of a sequence of $s + W$ instantons and s anti-instantons. Although these configurations are not true saddle point solutions, it can be shown that the interaction between instantons is weak³⁰ and the ideal (instanton) gas approximation may be used. Referring for a detailed account of the computation of the corresponding fluctuation determinant²⁸ to App. A 2, we here sketch the main steps.

Starting from the action (12), one expands in small fluctuations $\delta\phi$ around the instanton configuration $\phi_W(\{z\})$. We denote the Gaussian fluctuation contribution to the action by

$$\delta S_{\text{inst}} = g \langle \delta\phi | \hat{F}_W | \delta\phi \rangle,$$

where the linear operator \hat{F}_W is specified in the appendix. The spectrum of \hat{F}_W is given by

$$\lambda_m^{(W)} = \begin{cases} 0, & 1 \leq |m| \leq |W|, \\ |m| - |W|, & |W| < |m|. \end{cases}$$

To find Z_W , one has to integrate over the massive modes with eigenvalues $\lambda_m^{(W)}$ as well as over the zero modes z_a .

The massive mode integration leads to a reduction of the instanton action,

$$S_{\text{inst}} = \mathcal{G}_0 |W| \longrightarrow (\mathcal{G}_0 - \ln \frac{g E_c}{T}) |W|. \quad (16)$$

This “renormalization” of the coefficient \mathcal{G}_0 is analogous to the renormalization of the conductance in the Ohmic model discussed in Sec. II A (see Eq. (7).) In the present context it signals that instantons become increasingly important at low temperatures.

Finally, the integration over zero modes obtains a prefactor $\sim (g \ln E_c/T)^{|W|}$. Combining all contributions and accounting for combinatorial factors we thus obtain

$$\frac{Z_W}{Z_0} = \sum_{s=0}^{\infty} \frac{1}{(s + |W|)! s!} \left(\pi g^2 \frac{E_c}{T} e^{-\mathcal{G}_0} \ln \frac{E_c}{T} \right)^{2s + |W|}. \quad (17)$$

We finally sum over winding numbers W to obtain the instanton contribution to the free energy²⁸, $F = -T \ln Z$,

$$\delta F(q, T) = -2\pi g^2 E_c e^{-\mathcal{G}_0} \ln \frac{E_c}{T} \cos(2\pi q). \quad (18)$$

Charge quantization renders the free energy a periodic function of the gate voltage q . However, as expected, the amplitude is exponentially small in \mathcal{G}_0 .

Using the same formalism, we may compute the conductance $G(q)$ through the dot. As shown in App. A 3, the phase representation of the Kubo conductance is given by

$$G(q) = -2g^2 Z^{-1} \sum_W e^{2\pi i W q} \lim_{\omega \rightarrow 0} \frac{1}{\omega} \Im \left[\left\langle |\langle \delta\phi | \hat{F}_W | m \rangle|^2 \right\rangle_{S_W[\delta\phi]} \right]_{i\omega_m \rightarrow \omega + i0}. \quad (19)$$

Summing over instanton configurations, one obtains

$$G(q) = \frac{g}{2} \left(1 - \frac{\pi^3}{3} \frac{\tilde{E}_c}{T} \cos(2\pi q) \right), \quad (20)$$

where $\tilde{E}_c = g^2 E_c \exp[-\mathcal{G}_0]$ may be interpreted as an effective charging energy^{28,31}. As with the free energy, the conductance contains a weak gate voltage periodic modulation. Notice, however, that there is no zero-mode factor $\sim \ln E_c/T$. Rather, the massive mode integration leads to the much stronger divergence \tilde{E}_c/T .

The above approach is valid as long as the correction is small, i.e., $T \gg \tilde{E}_c |\cos(2\pi q)|$. At smaller temper-

atures, the instanton expansion becomes uncontrolled. The q -dependence of the corrections to the free energy and the conductance is linked to charge quantization. In the following, we shall study the same problem within the charge description. We will show that both models yield identical results, and point out a number of similarities and differences between the two approaches.

B. Charge model

Applied to a lead-dot-lead setup, the charge action Eq. (10) assumes the form

$$S[\theta] = \frac{1}{T} \sum_m \left(\sum_{i=L,R} \pi |\omega_m| \theta_{i,m}^2 + E_c (\theta_{L,m} - \theta_{R,m} - q \delta_{m,0})^2 \right) - \frac{D}{\pi} \sum_{i=L,R} r_i \int_0^\beta d\tau \cos(2\pi \theta_i(\tau)). \quad (21)$$

Generalizing to multi-channel contacts, we replace $r_i \rightarrow \exp[-\mathcal{G}_{i,0}/2]$. As long as $\mathcal{G}_{i,0} \gg 1$, one may treat the cosine-term perturbatively. Expanding to lowest non-vanishing order in $e^{-\mathcal{G}_{L,0}/2}$ and $e^{-\mathcal{G}_{R,0}/2}$, one obtains the contribution to the partition function

$$\frac{Z_1}{Z_0} = \frac{D^2}{2\pi^2} e^{-\mathcal{G}_0} \cos(2\pi q) \int d\tau d\tau' \Re \left\langle e^{2i\pi(\theta_L(\tau) - \theta_R(\tau'))} \right\rangle,$$

where $\mathcal{G}_0 = (\mathcal{G}_{L,0} + \mathcal{G}_{R,0})/2$.

Using that $\langle e^{i\hat{X}} \rangle = \exp[-\frac{1}{2}\langle \hat{X}^2 \rangle]$ and evaluating the correlators $\langle \theta_i \theta_j \rangle$, we thus obtain

$$\frac{Z_1}{Z_0} \sim E_c e^{-\mathcal{G}_0} \cos(2\pi q) \int d\tau d\tau' \frac{1}{|\tau - \tau'|} \quad (22)$$

$$= \frac{E_c}{T} e^{-\mathcal{G}_0} \ln \frac{E_c}{T} \cos(2\pi q). \quad (23)$$

This correction corresponds to the one-instanton correction to the phase model. In a similar manner, the inclusion of higher order terms yields the correction to the free energy²¹,

$$\delta F(q, T) = -\frac{8e^{\mathbf{C}} E_c}{\pi^3} e^{-\mathcal{G}_0} \ln \frac{E_c}{T} \cos(2\pi q), \quad (24)$$

where $\mathbf{C} \approx 0.577$ is the Euler constant.

The phase-dependent contribution δF matches the result obtained from the phase model, Eq. (18). Again, however, the approximations leading to this result are limited to temperatures higher than a certain cutoff temperature. Presently, however, we are in a position to explore what happens below that temperature:

At smaller temperatures, the cosine-potential itself provides a mass to the field θ . The relevant scale may be extracted by comparing the amplitude of the cosine-potential with the effective bandwidth — they become comparable at $T \sim \tilde{E}_c(q) = E_c e^{-\mathcal{G}_0} |\cos(2\pi q)|$. This temperature scale provides a cut-off for the logarithmic temperature-dependence of the free energy²¹. Thus, at temperatures $T < \tilde{E}_c(q)$, the correction to the free energy saturates at $\delta F(q, \tilde{E}_c(q))$.

Corrections to the conductance may be found in a similar way. As a result, one obtains^{21,32}

$$G = \frac{g}{2} \left(1 - \frac{e^{\mathbf{C}} E_c}{\pi T} e^{-\mathcal{G}_0} \cos(2\pi q) \right). \quad (25)$$

To exponential accuracy, and using $\tilde{E}_c \sim E_c e^{-\mathcal{G}_0}$, this is identical to the result (20) obtained from the phase model.

C. Comparison

In the previous two sections, we reviewed Coulomb blockade effects for a single quantum dot strongly coupled to the two leads.

In Sec. III A, we started from a microscopically derived phase action. We applied an instanton analysis to identify the ‘effective charging energy’ $\tilde{E}_c = g^2 E_c \exp[-\mathcal{G}_0]$. We also found that perturbation theory is applicable for temperatures $T > \tilde{E}_c |\cos(2\pi q)|$.

In Sec. III B, the starting point was a phenomenological model for the same system. The derivation of that model required the condition of weak backscattering in all channels, $r_\alpha \ll 1$. To exponential accuracy, a perturbative expansion in the reflection coefficients obtained results equivalent to those of Sec. III A. Again perturbation theory breaks down when the effective amplitude of the cosine-potential becomes of order of the bandwidth, $T \sim \tilde{E}_c |\cos(2\pi q)|$. At lower temperatures, the temperature dependence of the free energy saturates. The conductance, on the other hand, is suppressed and behaves as^{21,26} $(T/\tilde{E}_c(q))^2$.

As we shall demonstrate below, the equivalence of the phase and the charge description, respectively, will pertain to array-type geometries. However, as with the single quantum dot, the charge model will be preferable over the phase model when it comes to exploring low-temperature properties. Remarkably, for arrays the equivalence of the two descriptions may be demonstrated in explicit terms (and not just exemplified on specific observables as was the case for the single dot.) A second difference to the isolated dot regards the role of the cosine-potential of the charge model: While for a dot, a strong potential (of the order of the ‘bandwidth’) is required to impede charge fluctuations, in an array arbitrarily weak periodic potentials suffice to ‘pin’ spatial modulations^{10,11}. In fact, the efficiency of even weak potentials in impeding charge fluctuations will be at the root of the localization phenomenon in arrays.

IV. 1D ARRAY

We next advance to the 1d array geometry. As in the previous section, we start with the AES phase model (IV A) and then continue to the charge model (IV B).

A. Phase model

Our starting point is the generalization of Eqs. (3) and (4) to the 1d array geometry,

$$S_c[\phi] = \sum_{j=1}^M \int d\tau \left(\frac{\dot{\phi}_j^2}{4E_c} - iq\dot{\phi}_j \right), \quad (26)$$

$$S_t[\phi] = \frac{1}{16} \sum_{j=1}^{M-1} \sum_k \kappa_k \text{tr} \left[(\Lambda e^{i\delta\phi_j} \Lambda e^{-i\delta\phi_j})^k \right], \quad (27)$$

where M is the number of grains, and $\delta\phi_j = \phi_{j+1} - \phi_j$.

As in the single dot case, we shall focus on instanton phase configurations. Consider a configuration, where the phase on grain j_0 has an instanton, i.e., a winding number $W_{j_0} = 1$, whereas $W_j = 0$ everywhere else. The action of this configuration is given by $S_t = 2(\mathcal{G}_0/2)$ from the tunneling terms $j_0 \rightarrow j_0 \pm 1$ and $S_c = \pi^2 T/E_c$ from the charging term. Importantly, the fact that the tunneling action depends only on phase *differences* implies the existence of other instanton configurations of similar action: for example, the action of a sequence of $W = 1$ instantons on the grains $\{j_0, j_0 + L\}$ will again cost tunneling action $S_t = 2(\mathcal{G}_0/2)$ (from the tunneling terms $j_0 - 1 \rightarrow j_0$ and $j_0 + L \rightarrow j_0 + L + 1$.) Only the charging action depends in an extensive manner on the length L of the plateau: $S_c(L) = L\pi^2 T/E_c$. However, $\pi^2 T/E_c \ll 1$ whereas $\mathcal{G}_0 \gg 1$.

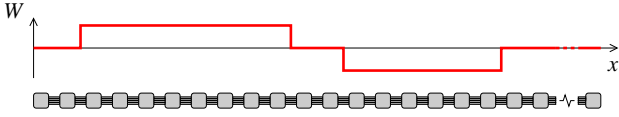


FIG. 2: (Color online) A typical configuration of the instanton winding numbers along the 1d array. The edges of the plateaus play the role of fictitious charges in the Coulomb gas mapping.

Thus, typical instanton configurations consist of long plateaus with a given winding number W that differs from the winding number of the background, W_b , by ± 1 .

(Ignoring the charging term, the action of a single plateau with height $|W - W_b| = 2$ equals that of two $|W - W_b| = 1$ plateaus. However, the latter configuration has the benefit of a much larger entropy which is why we will ignore the unlikely formation of configurations with step heights $|W - W_b| > 1$ throughout. The action of the phase model for a given configuration of winding numbers reads

$$S[W_j] = \sum_j \left(\frac{\pi^2 T}{E_c} W_j^2 + \frac{\mathcal{G}_0}{2} |W_j - W_{j-1}| \right). \quad (28)$$

The partition function is obtained by summing over all configurations $\{W_i\}$,

$$Z = \sum_{\{W_i\}} e^{-S[\{W_i\}]} \times (\text{fluctuation terms}). \quad (29)$$

One may rearrange the sum by introducing a new set of variables $\sigma_i = W_i - W_{i-1} \in \{-1, 0, 1\}$. Boundary conditions at the leads require $W_0 = W_{M+1} = 0$, i.e., σ_i obeys the sum rule $\sum_{i=1}^{M+1} \sigma_i = 0$. The contributions to the partition function from configurations $\{\sigma_i\}$ can be classified according to $\sum_i \sigma_i^2 = 2k$ (where the sum is even due to the neutrality condition $\sum_i \sigma_i = 0$.) We thus find

$$\begin{aligned} Z &= \sum_{\{\sigma_i\}} e^{\frac{\pi^2 T}{E_c} \sum_{j,j'} |j-j'| \sigma_j \sigma_{j'} - \frac{1}{2} \mathcal{G}_0 \sum_j \sigma_j^2} \\ &= \sum_{k=1}^{\infty} \left(e^{-\mathcal{G}_0/2} \right)^{2k} \sum_{\{\{\sigma_i\} | \sum_i \sigma_i^2 = 2k\}} e^{\frac{\pi^2 T}{E_c} \sum_{j,j'} |j-j'| \sigma_j \sigma_{j'}}, \end{aligned} \quad (30)$$

where we used that $|W_i - W_{i-1}| \rightarrow \sigma_i^2$ as well as

$$\sum_i W_i^2 = - \sum_i \sum_{j \leq i} \sigma_j \sum_{j' > i} \sigma_{j'} = -\frac{1}{2} \sum_{j,j'} |j-j'| \sigma_j \sigma_{j'}.$$

Since the action for $\sigma_i = 0$ is zero, it is sufficient to focus on non-zero charges $\sigma_i = \pm 1$ at positions x_i . Relabeling the σ_i , the summation over different configurations is replaced by an integration over the positions x_i of the charges σ_i . The corresponding partition function can be rewritten as

$$Z = \sum_{k=1}^{\infty} \left(e^{-\mathcal{G}(T)/2} \right)^{2k} \frac{1}{(k!)^2} \prod_{i=1}^{2k} \sum_{x_i=1}^M \exp \left[\frac{\pi^2 T}{E_c} \sum_{j,j'=1}^{2k} (-1)^{j+j'} |x_j - x_{j'}| \right], \quad (31)$$

i.e., as the partition function of a classical 1d neutral Coulomb gas with the fugacity $e^{-\mathcal{G}(T)/2}$ and effective charge $\pi T/\sqrt{E_c}$. Here we have replaced $\mathcal{G}_0 \rightarrow \mathcal{G}(T)$, anticipating that the integration over fluctuations around the stationary instanton configurations will lead to a

temperature-dependent renormalization of the conductance. As a result of a calculation conceptually similar to that for the isolated dot geometry (cf. App. A 2 b) we

indeed find that the fluctuation determinant is given by

$$\mathcal{F} = \exp \left[-\frac{2M}{M+1} \ln \frac{gE_c}{T} \right] = \left(\frac{T}{gE_c} \right)^{\frac{2M}{M+1}}. \quad (32)$$

The presence of this factor leads to the renormalization $\mathcal{G}_0 \rightarrow \mathcal{G}(T) = \mathcal{G}_0 - \frac{2M}{M+1} \ln(gE_c/T)$ implied in Eq. (31). Notice that for a long array $M \rightarrow \infty$ the renormalization is more significant than for a single grain, $M = 1$.

It is well known (see App. A 4) that the 1d Coulomb gas, Eq. (31), is equivalently described by the action of the 1d discrete sine-Gordon model

$$S[\theta] = \sum_j \left\{ \frac{E_c}{T} (\theta_{j+1} - \theta_j)^2 - 2e^{-\mathcal{G}(T)/2} \cos(2\pi\theta_j) \right\}. \quad (33)$$

Introducing the parameter

$$\gamma = 4\pi^2 g e^{-\mathcal{G}_0/2} \ll 1, \quad (34)$$

and using that $e^{-\mathcal{G}(T)/2} = (gE_c/T)e^{-\mathcal{G}_0/2}$ this action may be reformulated as

$$S[\theta] = \frac{E_c}{T} \sum_j \left\{ (\theta_{j+1} - \theta_j)^2 - \frac{\gamma}{2\pi^2} \cos(2\pi\theta_j) \right\}. \quad (35)$$

Before discussing the physics of this model, we will derive it in an alternative manner, viz. from the charge model. This will make the equivalence of the charge and the phase description explicit, and elucidate the physical meaning of the field θ .

B. Charge model

The straightforward generalization of the charge action Eq. (10) to a 1d array of dots is given by

$$S[\theta] = \sum_j \left\{ \frac{1}{T} \sum_m (E_c(\theta_{j+1,m} - \theta_{j,m} - q\delta_{m,0})^2 + \pi|\omega_m|\theta_{j,m}^2) - \frac{Dr}{\pi} \int d\tau \cos(2\pi\theta_j) \right\}. \quad (36)$$

Thermodynamic properties of the array may be probed by differentiation with respect to the gate voltage q . Noting that q couples only to the static sector of the field $\theta_{j,0} = \int d\tau \theta_j(\tau)$, one may try integrate out all non-zero Matsubara components $\theta_{j,m \neq 0}$ at an early stage of the analysis. To this end let us write

$$\theta_j(\tau) = \theta_{j,0} + \delta\theta_j(\tau). \quad (37)$$

In the quadratic part of the action θ_0 and $\delta\theta$ decouple. Denoting the average over the quadratic $\delta\theta$ -action by $\langle \dots \rangle$, we approximate the functional integral over the anharmonic part of the action by $\langle \exp(\int \cos\theta) \rangle \simeq \exp \int \langle \cos\theta \rangle$, i.e.,

$$\begin{aligned} \langle \cos(2\pi\theta) \rangle_{m \neq 0} &\rightarrow \frac{1}{2} (e^{i2\pi\theta_0} \langle e^{i2\pi\delta\theta} \rangle + e^{-i2\pi\theta_0} \langle e^{-i2\pi\delta\theta} \rangle) \\ &= \cos(2\pi\theta_0) \exp[-2\pi^2 \langle \delta\theta^2 \rangle]. \end{aligned} \quad (38)$$

Performing the integral over $\delta\theta$, we find

$$\langle \delta\theta^2 \rangle = \frac{T}{2M} \sum_{|\omega_m| \neq 0} \sum_p \frac{1}{E(p) + \pi|\omega_m|} = \frac{1}{2\pi^2} \ln \frac{D}{e^C E_c}, \quad (39)$$

where $E(p) = 4E_c \sin^2(p/2)$ is the lattice dispersion. Importantly, Eq. (39) does not contain temperature-dependent infra-red singularities. This provides the a posteriori justification of the above integration procedure. Substituting the $\delta\theta$ -averaged cosine operator back

into the action of the static field we obtain

$$S_{\text{cl}} = \frac{E_c}{T} \sum_{j=1}^{M-1} \left\{ (\theta_{j+1,0} - \theta_{j,0} - q)^2 - \frac{\gamma}{2\pi^2} \cos(2\pi\theta_{j,0}) \right\}, \quad (40)$$

where $\gamma = 2\pi e^C r$. As shown in appendix B 1, generalization to the multi-channel case amounts to the substitution $\gamma = 2\pi e^C \prod_{\alpha} r_{\alpha} \sim e^{-\mathcal{G}_0/2}$.

To exponential accuracy, this result is equivalent to the action Eq. (35) obtained from the Coulomb gas representation of the phase model.

C. Thermodynamics of 1d arrays

In the previous sections, we have shown that the long-range physics of the granular array is effectively described by a classical model with free energy $F = TS_{\text{cl}}$, where

$$F(q) = E_c \sum_j \left\{ (\theta_{j+1} - \theta_j - q)^2 - \frac{\gamma}{2\pi^2} \cos(2\pi\theta_j) \right\}, \quad (41)$$

and the field index ‘0’ has been dropped for convenience.

This model is known as the discrete sine-Gordon model or, in the context of the adsorption of atoms on a periodic substrate, as the Frenkel-Kontorova model³³. [The Frenkel-Kontorova model describes a harmonic elastic chain of “atoms” with stiffness E_c , placed on top of a periodic “substrate” potential of amplitude $\gamma E_c/(2\pi^2)$. See Fig. 3.] In the following, we will summarize the physical

properties of this model, and translate to the context of the 1d quantum dot array.

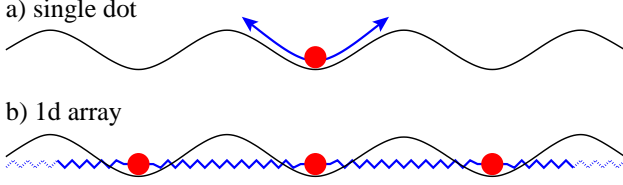


FIG. 3: (Color online) Chain of particles (each representing one quantum dot) subject to a shallow cosine-potential. While an isolated particle would experience no more than a weak back-scattering effect, a particle chain is subject to strong pinning. This leads to the appearance of a new (pinning) temperature scale $T^* \gg T_0$ which does not exist for single dots.

In the absence of a gate voltage ($q = 0$), the ground state of the chain is described by $\theta_j = 0$ for all j . This field describes a zero charge configuration. Charge excitations correspond to non-vanishing solutions extremizing the free energy F . Varying the action one finds that these configurations are given by

$$\bar{\theta}_j = \frac{2}{\pi} \arctan[\exp\{\sqrt{\gamma}(j - j_0)\}]. \quad (42)$$

Eq. (42) describes a solitary excitation centered at coordinate j_0 and extended over a scale $\xi_s = 1/\sqrt{\gamma} \gg 1$. The total charge carried by this excitation is quantized and given by $\mathcal{N}_{\text{tot}} = \sum_j (\theta_{j+1} - \theta_j) = \theta_{M+1} - \theta_1 = 1$. (Due to the large inter-grain tunneling,) it is spread over a large number $\gamma^{-1/2} \sim e^{\mathcal{G}_0/4}$ of grains.

Substituting this solution into the free energy (41), one obtains the soliton energy

$$T^* = E_c \sqrt{\gamma} \gg T_0. \quad (43)$$

At finite temperatures, the system will host a gas of thermally excited solitons and anti-solitons with density $n_s \sim \exp[-T^*/T]$. Due to the absence of gapless charge carriers in the system, transport will exhibit activation behavior, as we will show below.

At finite gate voltage, the uniform configuration $\theta_j = 0$ will acquire the finite energy $\delta F_{\text{el}}(q) = M E_c q^2$ (the elastic term in the action.) By contrast, the configuration $\theta_j = j q$ which minimizes the elastic term has the energy $\delta F_{\text{pot}}(q) = -M E_c \gamma / (2\pi^2)$ (the cosine-potential.) The smaller of the two determines the ground state of the system. In the language of the Frenkel-Kontorova model, the “incommensurability parameter” q represents the periodicity mismatch between the chain and the substrate. For small values of q the system will find it favorable to retain a commensurate state, i.e., the chain will stretch a little so as to still benefit from an optimal coupling to the substrate. Thus, the system remains in a commensurate phase $\theta_j = 0$ for gate voltages $q < q^* = \sqrt{\gamma/(2\pi^2)}$. At q^* , where the two energies

become equal ($\delta F_{\text{el}}(q^*) = \delta F_{\text{pot}}(q^*)$), a commensurate-incommensurate transition takes place — at this gate voltage solitons are created at no cost. For the average number of electrons per grain, $\bar{N}(q) \equiv q - \partial_q F / (2M E_c)$, one thus expects: $\bar{N}(q) = 0$ for $|q| \leq q^*$ (insulator) and $\bar{N}(q) \rightarrow q$ for $|q| > q^*$ (metal).

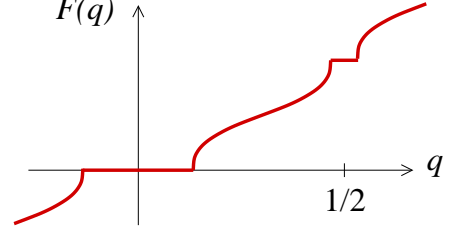


FIG. 4: (Color online) Free energy of the 1d array as function of the common background charge, q . Only two insulating plateaus at $q = 0$ and $q = 1/2$ are shown.

A more thorough discussion of the system (cf. Ref. [33]) shows that insulating ‘plateaus’ along with superimposed solitary excitations form not only around $q = 0$, but also around other rational values of q . However, both the width of these plateaus and the corresponding activation energies decrease for higher rational fractions. Among the low-lying rationals, $q = 1/2$ plays a particularly interesting role. Indeed, for a *single* grain, $q = 1/2$ represents the charge degeneracy point, where the system is in a conducting state (Coulomb blockade peak). Unexpectedly, the *array* exhibits a very different behavior. Using the language of the Frenkel-Kontorova model, $q = \pm 1/2$ is special in that the atoms of the unperturbed chain alternately find themselves in minima/maxima of the substrate potential. Under these conditions, energy can be gained by a ‘Peierls-distortion’, doubling the period, i.e., a density modulation with amplitude $\delta\theta_j \sim \gamma$. This configuration does not respond to small variations in q — corresponding to insulating behavior. However, the width of the insulating plateau $\Delta q_{1/2} \sim \gamma$ is much smaller than the width of the plateau $\Delta q_0 \equiv 2q^* \sim \sqrt{\gamma}$ at $q = 0$. The dependence of the free energy on q (including the two plateaus) is shown in Fig. 4.

D. DC transport

In order to discuss the DC conductivity of the array, one needs to restore the low-frequency, $\omega \ll T$, dynamics of the classical charge model, Eq. (41). In principle, this may be done by keeping the dissipative term in the action. It turns out that in the multi-channel case (cf. App. B 1), and for strong backscattering, the coefficient of the dissipative term reads as $\pi g^{-1} |\omega_m| \theta_{j,m}^2$. While this seems to satisfactorily describe the dynamics of Ohmic dissipation, the main drawback of the imaginary time approach is that it involves cumbersome analytical continuations $\omega_m \rightarrow \omega + i0$. To avoid this complication, it is convenient to pass to the Keldysh representation. In fact,

it turns out to be sufficient to focus on the semi-classical limit of the Keldysh formalism, i.e., a limit physically equivalent to a description of the system in terms of a classical Langevin equation³⁴. Referring for a more detailed discussion of these connections to App. B 2, we here take the adequacy of this formulation for granted and describe the system in terms of the Langevin equation right away:

To start with, consider the equations of motion of the static model, Eq. (41): $\partial(\frac{e}{C}\partial\theta_j) - \frac{e\gamma}{2\pi C}\sin(2\pi\theta_j) = 0$. Since $\frac{e}{C}\partial\theta_j \equiv V_j$ is the voltage on grain j , this equation simply expresses the fact that in the absence of charge quantization, $\gamma \rightarrow 0$, all grains are equipotential: $\partial V_j = V_{j+1} - V_j = 0$. We now ask how these equations have to be modified if currents are allowed to flow. The minimal classical description of dissipative current flow between grains $j+1$ and j is provided by the current-voltage relation $V_{j+1} - V_j = RI_j$, where $R = 2\pi\hbar/(e^2g)$ is the contact resistance, and $I_j = e\partial_t\theta_j$ the current flowing between grains j and $j+1$. Restoring the γ -term, we are led to the phenomenological generalization of the equation above,

$$\frac{\pi}{g}\partial_t\theta - E_c\left[\partial^2\theta - \frac{\gamma}{2\pi}\sin(2\pi\theta)\right] = -\frac{e}{2}E + \xi(t), \quad (44)$$

where we have introduced a Gaussian noise term, $\xi(t)$, with the correlator

$$\langle \xi_j(t)\xi_{j'}(t') \rangle = \frac{2\pi T}{g}\delta(t-t')\delta_{j,j'}, \quad (45)$$

to satisfy the fluctuation-dissipation theorem, and an external electric field, E , as a driving source of current. Formally, Eq. (44) represents a Langevin equation for the classical degree of freedom, θ .

Our goal is to calculate the current, I , driven by a weak uniform field, E . As we saw above, charge transport in the present model is by solitary excitations. As an ansatz for the current we thus use $I = en_s v$, where n_s is the soliton concentration and v is their effective drift velocity. While the soliton concentration, n_s , has been discussed above, the drift velocity still needs to be determined. To this end, we temporarily ignore the noise term and seek for propagating solutions of Eq. (44). Assuming the external field to be weak, we consider the ansatz $\theta(j, t) = \bar{\theta}(j - vt) + \theta_1(j - vt) + \zeta$, where $\bar{\theta}$ is the static soliton, $\theta_1 \sim E$ a small distortion of the soliton shape due to the presence of the external field, and the constant ζ accounts for the weak shift of the minimum of the periodic potential by the field: $E_c\gamma\sin(2\pi\zeta) = \pi E$. Linearizing Eq. (44), we find that θ_1 satisfies the equation

$$E_c\hat{\mathcal{L}}_{\{\bar{\theta}\}}\theta_1 = \frac{v}{g}\partial\bar{\theta} - \frac{E}{\pi}\sin^2(\pi\bar{\theta}), \quad (46)$$

where $\hat{\mathcal{L}}_{\{\bar{\theta}\}} \equiv \partial^2 - \gamma\cos(2\pi\bar{\theta})$. Importantly, it is not our prime objective to identify the actual shape of the soliton (θ_1); Rather, we wish to compute its speed of propagation, v . An equation for v may be obtained by noting

that θ_1 has been introduced to describe a change in the *shape* of the soliton in response to the field. This needs to be distinguished from the temporal change in its *position* (which has been accounted for by the introduction of the as yet undetermined shift vt .) To discriminate between these two effects, we require that the linear equation determining θ_1 be an equation in a function space orthogonal to the zero mode function, $\partial\bar{\theta}$, describing translations of the soliton, $\bar{\theta}(x + \delta x) - \bar{\theta}(x) \sim \delta x\partial\bar{\theta}$. In particular, v should be determined in such a way that the r.h.s. of the equation be orthogonal to $\partial\bar{\theta}$,

$$\int dx \left(\frac{v}{g}\partial\bar{\theta} - \frac{E}{\pi}\sin^2(\pi\bar{\theta}) \right) \partial\bar{\theta} = 0. \quad (47)$$

Using Eq. (42) for $\bar{\theta}$, this requirement leads to the expected result $v \sim gE$. This in turn implies that the DC conductivity is given by $\sigma = gn_s(T)$. Using that for low temperatures, $T < T^*$, the soliton density shows activation behavior, $n_s(T) \sim \exp[-T^*/T]$, we arrive at the result Eq. (1).

E. Density of states

As another quantity of interest we discuss the (tunneling) density of states. At large energies, the density of states can be conveniently described within the phase model. Within the framework of that model, the DoS $\nu(\epsilon) = -\frac{1}{\pi}\Im \text{tr}[G(i\omega_m)]|_{i\omega_m \rightarrow \omega + i0}$ is represented as

$$\nu(\epsilon) = \nu_0 T \Im \int d\tau \frac{e^{i\epsilon_n\tau}}{\sin\pi T\tau} \left\langle e^{i\sum_q(\phi_q(\tau) - \phi_q(0))} \right\rangle \Big|_{i\epsilon_n \rightarrow \epsilon^+}. \quad (48)$$

At large temperatures, the ‘Debye-Waller factor’ $\left\langle e^{i\sum_q(\phi_q(\tau) - \phi_q(0))} \right\rangle \simeq \exp[-\frac{1}{2}\sum_q\langle|\phi_q(\tau) - \phi_q(0)|^2\rangle]$ may be computed from the quadratic approximation to the phase action. This leads to

$$\begin{aligned} \sum_q \langle |\phi_q(\tau) - \phi_q(0)|^2 \rangle &= 4T \sum_{q,m} \frac{1 - \cos\omega_m\tau}{|\omega_m|(\frac{g}{\pi}q^2 + \frac{|\omega_m|}{E_c})} \\ &= 2\sqrt{2\frac{E_c\tau}{g}}. \end{aligned} \quad (49)$$

Integrating over τ and performing the analytic continuation we thus obtain the result

$$\nu(\epsilon) \sim \nu_0 \exp\left[-\sqrt{2\frac{E_c}{g\epsilon}}\right]. \quad (50)$$

Notice that the conductivity and the DoS, respectively, are governed by different energy scales. The DoS becomes exponentially small at energies $\epsilon \sim E_c/g \gg T^*$. To understand what happens below that energy, notice that the minimal energy required to add a charge to the array is the excitation energy of a soliton. Therefore, at zero temperature, the DoS vanishes at energies smaller

than T^* ; i.e. $\nu(\epsilon < T^*) = 0$. The charge quantization leads to a hard gap in the DoS.

This concludes our discussion of the one-dimensional array. We have found that the proliferation of instantons at low temperatures drives the system into an insulating phase where transport is activated and conducted by the charge solitons. The temperature at which activation behavior sets in is exponentially small in the dimensionless conductance. Yet it is parametrically larger than the scale T_0 where the perturbative corrections become large: $T^*/T_0 \sim e^{\mathcal{G}_0/4} \gg 1$. The tunneling DoS is significantly suppressed at even higher energies and displays a hard gap at the soliton energy.

V. 2D ARRAYS

We next extend our discussion to two-dimensional quantum dot arrays. Our strategy will parallel that of the previous sections: Starting from the phase representation we will establish a connection to the complementary charge representation, and then discuss the physics of the system in terms of the latter.

A. Phase model

Again we start from the action (3) and (4), where the lattice summation now extends over a two-dimensional regular array. Anticipating the importance of ‘winding numbers’, we begin with an identification of instanton solutions right away. As depicted in Fig. 5, instanton configurations in the 2d geometry assume the form of “islands”, i.e., regions of a certain winding number W_{island} surrounded by a background with a different winding number W_b . For entropic reasons, configurations with $W_b = 0$ and $W_{\text{island}} = \pm 1$ will dominate. The action of one such island of area A and circumference L is given by $S_{\text{island}} = \frac{\pi^2 T}{E_c} A + \frac{\mathcal{G}_0}{2} L$. For an island differing by a generic winding number from its background, this generalizes to

$$S_{\text{island}} = \frac{\pi^2 T}{E_c} A W^2 + \frac{\mathcal{G}(T)}{2} L |W|, \quad (51)$$

where we anticipated that the inclusion of fluctuations will again manifest itself in a renormalization of the conductance, $\mathcal{G}_0 \rightarrow \mathcal{G}(T)$.

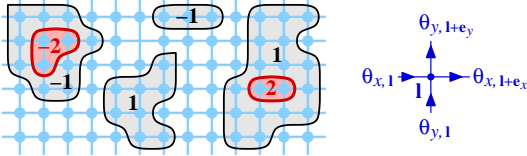


FIG. 5: (Color online) The “islands” with fixed values of the winding number in a 2d array. The area $A = 1, 2, \dots$ is the number of grains inside an island, while the circumference $L = 4, 6, 8, \dots$ is the number of links crossed by its boundary.

As a result of a straightforward generalization of the one-dimensional fluctuation determinant discussed in App. A 2b, we indeed find (cf. App. A 2c) that the determinant due to fluctuations around the stationary configuration is given by

$$\mathcal{F} = \exp \left[-\frac{L}{2} \ln \frac{gE_c}{T} \right] = \left(\frac{T}{gE_c} \right)^{\frac{L}{2}}. \quad (52)$$

We account for the presence of this factor by renormalization $\mathcal{G}_0 \rightarrow \mathcal{G}(T) \equiv \mathcal{G}_0 - (2/d) \ln(gE_c/T)$, where $d = 2$. (In fact, it is straightforward to verify that this result holds for systems of arbitrary dimensionality.)

B. Charge model

Starting from Eq. (10) (where the sum now extends over a 2d array), our strategy will be to successively integrate over high-frequency fluctuations to derive an effective low-energy action. (Unlike in the 1d case where all dynamical fluctuations could be integrated out in one sweep.) Consider, thus, fluctuations of $\vec{\theta}(\tau)$ in a window of (Matsubara) energies between the bandwidth D and $\tilde{D} < D$. Integration over these fluctuations will lead to a renormalization of the cosine-potential. As long as the renormalized backscattering amplitude is small, functional averages over high frequency fluctuations can be taken using the quadratic action.

Due to the vector nature of $\vec{\theta}$, there are two types of modes contributing to the fluctuations. Using the representation $\vec{\theta} = \nabla\chi + \nabla \times \eta$, where χ and η are scalar fields and ∇ and $\nabla \times$ lattice variants of gradient and curl, respectively, the charging action takes the η -independent form $S_c[\chi, \eta] = E_c \sum_{\mathbf{l}} (\nabla\chi_{\mathbf{l}})^2 / T$. The Gaussian average

$$\langle \theta_i^2 \rangle_f = \frac{1}{2\pi} \sum_{\mathbf{p}} T \sum_{\tilde{D} < |\omega_m| < D} \left(\frac{1}{|\omega_m|} + \frac{\pi}{E(\mathbf{p}) + \pi|\omega_m|} \right),$$

thus splits into two contributions, where only one (the χ -contribution) couples to the lattice dispersion $E(\mathbf{p}) = 4E_c(\sin^2 \frac{p_x}{2} + \sin^2 \frac{p_y}{2})$. For frequencies $\tilde{D} < E_c$, we find

$$\langle \theta_i^2 \rangle_f = \frac{1}{4\pi^2} \ln \frac{D^2}{E_c \tilde{D}}, \quad (53)$$

i.e., the χ -mode is effectively frozen out due to its coupling to the charging action. However, (and unlike in the 1d-case) there is one “massless” mode whose fluctuation amplitude depends on the effective bandwidth \tilde{D} . Using this result to renormalize the coefficient of the cosine-potential we obtain

$$D e^{-\mathcal{G}_0/2} \rightarrow \sqrt{E_c \tilde{D}} e^{-\mathcal{G}_0/2}. \quad (54)$$

This integration procedure can be iterated until the renormalized backscattering amplitude is of order of the

bandwidth, i.e., $\tilde{D} \sim E_c e^{-\mathcal{G}_0} \equiv T_0$, corresponding to an effective conductance $\mathcal{G}_{\text{eff}} = \mathcal{O}(1)$. For temperatures $T > T_0$, (i.e., for a Matsubara frequency spacing $\sim T$ larger than the cutoff energy) one may approximate the action by the zero Matsubara (classical) contribution

$$S_{\text{cl}}[\vec{\theta}] = \frac{E_c}{T} \sum_{\mathbf{l}} \left\{ (\nabla \cdot \vec{\theta}_{\mathbf{l}})^2 - \frac{\gamma(T)}{2\pi^2} \sum_{i=x,y} \cos(2\pi\theta_{i,\mathbf{l}}) \right\}, \quad (55)$$

where $\gamma(T) = 2\pi\sqrt{T/E_c}e^{-\mathcal{G}_0/2}$.

At smaller temperatures $T < T_0$, all modes become massive due to the cosine-term. This leads to a saturation of the coefficient $\gamma(T)$,

$$\gamma(T) \sim \begin{cases} \sqrt{T/E_c}e^{-\mathcal{G}_0/2} & T > T_0, \\ \sqrt{T_0/E_c}e^{-\mathcal{G}_0/2} \simeq e^{-\mathcal{G}_0} & T < T_0. \end{cases} \quad (56)$$

We shall show now that the perturbative expansion in powers of $\gamma(T)$ of the classical model, Eq. (55), leads to the same island scenario discussed above within the phase model.

For bookkeeping purposes, we label the coefficients $\gamma_{\underline{\alpha}}(T)$ by the index of the bond $\underline{\alpha} = (i, \mathbf{l})$ ($i = x, y$) to which they belong. The partition function can then be written as

$$Z = \sum_{n=0}^{\infty} Z_n (E_c/T)^n \prod_{\substack{\underline{\alpha}_j \\ (j=1 \dots n)}} \gamma_{\underline{\alpha}_j}(T),$$

where Z_n is a product of n cosine-terms averaged over the quadratic action $S_c[\vec{\theta}] = E_c \sum_{\mathbf{l}} (\nabla \cdot \vec{\theta}_{\mathbf{l}})^2 / T$. Two types of contributions to this expansion can be distinguished: a) terms containing higher powers of the cosine taken at the same link and b) terms involving different links. One may show that the first class of terms describes perturbative corrections to the conductance of a single contact (equivalent to those obtained in Ref. [9] within the framework of the phase model.) We here focus on the phenomenon of “island formation”, as described by the second family, b).

The expansion of Z_n generates expressions of the form $\exp[2\pi i (\sum_{j_x=1}^s (\pm)\theta_{x,\mathbf{l}_{j_x}} + \sum_{j_y=s+1}^n (\pm)\theta_{y,\mathbf{l}_{j_y}})]$, where j_i labels contacts in i -direction. To perform the θ -average, we again use the representation $\vec{\theta} = \nabla\chi + \nabla \times \eta$. While the fields χ are defined on the lattice, the fields η are defined on the reciprocal lattice (see Fig. 6.) Importantly, the (now classical) rotational field η is strictly massless. This means that contributions to the expansion containing an uncompensated η -amplitude in the exponent average to zero. The surviving terms obey the condition $\sum_{j_x} \pm(\eta_{\mathbf{l}_{j_x}+\mathbf{e}_y} - \eta_{\mathbf{l}_{j_x}}) + \sum_{j_y} \mp(\eta_{\mathbf{l}_{j_y}+\mathbf{e}_x} - \eta_{\mathbf{l}_{j_y}}) = 0$. This corresponds to the island structure: the lowest-order non-local term is proportional to $\gamma^4 = \gamma_{x,\mathbf{l}\gamma_{x,\mathbf{l}+\mathbf{e}_x}}\gamma_{y,\mathbf{l}\gamma_{y,\mathbf{l}+\mathbf{e}_y}}$ — involving all the four links surrounding grain \mathbf{l} .

Every island is weighted by a factor $(E_c\gamma(T)/T)^L$, where L is the order in perturbation theory required

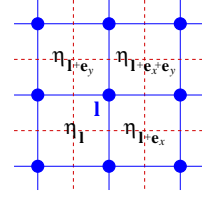


FIG. 6: (Color online) The rotational field η . The lattice curl is given as $(\nabla \times \eta)_{\mathbf{l}} = \begin{pmatrix} \eta_{\mathbf{l}+\mathbf{e}_y} - \eta_{\mathbf{l}} \\ -\eta_{\mathbf{l}+\mathbf{e}_x} + \eta_{\mathbf{l}} \end{pmatrix}$. Going around one grain, the η -fields coming from the 4 links cancel — thus, yielding a non-vanishing contribution to the expansion in γ .

for its formation. For an island with winding number $|W| = 1$, L is the lattice circumference. Islands with $|W| > 1$ are surrounded by a chain of γ -amplitudes $|W|$ times; in this case, $L = |W| \times \text{circumference}$. Finally, the averaging over the massive χ -fields results in a factor $\exp[-\pi^2 T A W^2 / E_c]$, where A is the island area.

Summarizing, every island carries a factor $\tilde{P}_W(A, L) = (e^{-\pi^2 T / E_c})^{A W^2} (E_c \gamma(T) / (2\pi^2 T))^{L|W|}$. Using Eq. (56), one finds that in the high-temperature regime, $T > T_0$, $E_c \gamma(T) / (2\pi^2 T) \simeq e^{-\mathcal{G}(T)/2}$. Thus, $\tilde{P}_W(A, L) = \exp[-\pi^2 (T/E_c) A W^2 - \frac{1}{2} \mathcal{G}(T) L |W|]$, which is in perfect agreement with the prediction of the phase model, cf. Eq. (51). At lower temperature, non-linear fluctuation corrections in the phase model diverge⁹ and the non-interacting instanton treatment runs out of validity. However, having established the equivalence of the phase and the charge model at $T > T_0$, one may proceed with the analysis of the latter even at smaller temperatures.

C. Solitons and the BKT crossover

In order to extract the low-temperature behavior of the array, we investigate the properties of the classical model (55). The lowest energy configuration of the action is given by the homogeneous solution $\vec{\theta} = 0 \pmod{1}$ everywhere. In order to minimize the cosine-potential, localized excitations must have integer $\vec{\theta}$ far away from the core. Since the total charge of such a localized excitation is $e \int (d^2 l) \nabla \cdot \vec{\theta} = e \int d\vec{s} \cdot \vec{\theta}$, where the line integral on the r.h.s. is calculated over a distant contour enclosing the excitation, the charge of the excitation is quantized in integer multiples of e . Excitations of lowest energy have charge $\pm e$. They consist of a large (i.e., spread out over $\sim 1/\gamma \sim e^{\mathcal{G}_0} \gg 1$ grains — see below) localized 2d soliton, connected to a 1d string of links with $\theta_i = 1$. The other end of the string may either go to the system boundary, or terminate in an anti-soliton of opposite charge. The soliton solution centered at $\mathbf{l} = 0$ can be written in the form $\vec{\theta}_{\mathbf{l}} = 1 - \vec{\vartheta}(\mathbf{l})$ for the links along the string and $\vec{\theta}_{\mathbf{l}} = \vec{\vartheta}(\mathbf{l})$ everywhere else, where $|\vec{\vartheta}(|\mathbf{l}| \rightarrow \infty)| \rightarrow 0$. Minimization of the action, Eq. (55), with respect to $\vec{\vartheta}$ yields the saddle point equation for the

soliton solution,

$$\nabla(\nabla \cdot \vec{\vartheta}) - \frac{\gamma(T)}{2\pi} \sum_{i=x,y} \sin(2\pi\vartheta_i) \mathbf{e}_i = 0. \quad (57)$$

Except for a domain consisting of $\mathcal{O}(1)$ links closest to the core of the soliton, ϑ is small, justifying an expansion of the sine-term in the saddle point equation, i.e., $\nabla(\nabla \cdot \vec{\vartheta}) - \gamma\vec{\vartheta} = 0$. Its unit-charge solution is

$$\vec{\vartheta}(\mathbf{l}) = -\frac{\sqrt{\gamma}}{2\pi} K_1\left(\frac{l}{\xi_s}\right) \mathbf{e}_l, \quad (58)$$

where $\mathbf{e}_l \equiv \mathbf{l}/l$ and K_1 is a modified Bessel function. The large size of the soliton, $\xi_s = 1/\sqrt{\gamma(T)} \gg 1$, justifies the continuum approximation.

To obtain the soliton energy T^* , we substitute this solution back into the action, Eq. (55). One finds that the energy originates primarily from the cosine-potential part and is given by $T^* = (E_c\gamma(T)/(2\pi)) \ln \xi_s$. The large factor $\ln \xi_s = -\frac{1}{2} \ln \gamma(T) \gg 1$ is due to the logarithmic spreading of the charge density over the wide range of distances $1 < l < \xi_s$. Due to this factor $T^* \gg T_0 \sim E_c\gamma(T_0)$ (while their ratio is exponentially large in g in 1d, here it is only algebraic.) At larger distances, $l > \xi_s$, the charge density decays exponentially.

The charge spreading leads to a long-ranged soliton-soliton interaction. The solitons interact logarithmically up to a distance ξ_s beyond which the interaction is exponentially screened. Since the density of thermally-excited solitons is $n_s \approx \exp[-T^*/T]$, the mean distance between them is $l_s = n_s^{-1/2} \approx \exp[T^*/(2T)]$ which becomes comparable to ξ_s at $T \approx T^*/(2 \ln \xi_s) = E_c\gamma(T)/(4\pi)$. This condition is satisfied at temperatures about the “freezing” temperature, $T \sim T_0$. Thus, at $T < T_0$, the thermally-excited charges are essentially non-interacting, while, at $T > T_0$, there is a neutral (in average) gas of logarithmically interacting solitons and anti-solitons. The soliton core energy yields the fugacity f of the logarithmic gas: $\ln f \simeq E_c\gamma(T)/T$.

In the latter regime the partition function of the charged degrees of freedom may be written as

$$Z = \sum_{n=0}^{\infty} \frac{f^n}{n!} \int (d^2l_1) \dots (d^2l_n) e^{\pm \frac{E_c\gamma(T)}{2\pi T} \sum_{k,k'} \ln |l_k - l_{k'}|}. \quad (59)$$

The plus/minus signs in the exponent correspond to soliton-soliton and soliton-anti-soliton interactions, respectively.

It is well known that the Coulomb gas in 2d described by Eq. (59) undergoes the BKT transition^{16,17} at a critical temperature $T_{\text{BKT}} \approx E_c\gamma(T_{\text{BKT}})/(4\pi)$. For $T < T_{\text{BKT}}$, the charges are bound in charge-anti-charge pairs. In this regime, the finite interaction range ξ_s leads to an exponentially small residual density of free charges $n_s \approx \exp[-T^*/T]$, where $T^* = T_{\text{BKT}} \ln(\xi_s^2)$. Above the transition/crossover temperature the density of free charges rapidly increases as¹⁶

$n_s \sim \exp[-2b\sqrt{T_{\text{BKT}}/(T - T_{\text{BKT}})}]$, where b is a constant of order unity, driving the array into the conducting phase.

Notice that the Coulomb interactions in our model are strictly on-site (only the self-capacitance, C , is included.) The long range of the soliton-soliton interactions is due to the fact that in a strongly coupled array, $\mathcal{G}_0 \gg 1$, the charge is spread over a large distance $\xi_s \sim \exp[\mathcal{G}_0/2]$. To describe the truly long-range Coulomb interactions, one may modify the model by including mutual capacitances C' between neighboring grains. It is straightforward to show that such modification alters the range of logarithmic interactions as $\xi_s \rightarrow \xi_s \sqrt{1 + C'/C}$, while the charging energy now reads $E_c = e^2/(2(C + C'))$. In the limit $C \rightarrow 0$, while C' remains finite, the interaction range diverges, $\xi_s \rightarrow \infty$, i.e., one deals with the true (logarithmic) 2d Coulomb interaction (without the self-capacitance no electric field lines can leave the system.) In this case, one observes a genuine BKT phase transition: $\xi_s \rightarrow \infty$ and the density of free charges below T_{BKT} becomes strictly zero.

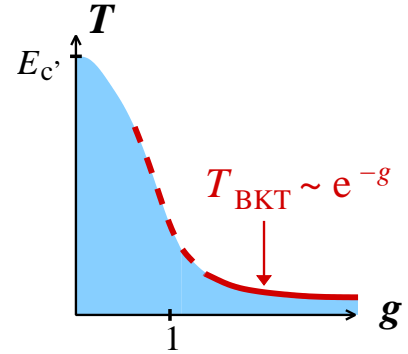


FIG. 7: (Color online) Phase diagram of the 2d granular array. The thick line indicates the BKT crossover temperature at $g > 1$. At smaller g the crossover disappears (in the self-capacitance model.) The shaded area indicates the region with exponentially small conductivity.

The conductivity of the array may be evaluated in the same way as in the 1d case. With the soliton velocity $v \sim gE$, one finds $\sigma \simeq g \exp[-T^*/T]$ at temperatures below T_{BKT} . Above T_{BKT} , the conductivity behaves³⁵ as $\sigma \simeq g \exp[-2b\sqrt{T_{\text{BKT}}/(T - T_{\text{BKT}})}]$, whereas, at even higher temperatures, this behavior crosses over to the result⁹ of the perturbative calculation, $\sigma = g - \ln(gE_c/T)$.

The corresponding phase diagram is shown in Fig. 7. Unlike previous works^{3,18,23} that predicted a zero-temperature metal for $g > g_c \simeq 1$, we find that the low-temperature phase is an insulator for arbitrarily large g . The critical temperature, $T_{\text{BKT}}(g)$, however, drops sharply at $g \simeq 1$ and, at large $g \gg 1$, behaves as $T_{\text{BKT}} \sim E_cg \exp[-\mathcal{G}_0]$.

D. Finite gate voltage

So far we have restricted ourselves to the case of zero gate voltage only. A finite gate voltage induces a continuous background charge $q \propto V_{\text{gate}}$ on the grains. In this case the charging term in the action Eq. (55) has to be replaced with $S_{\text{cl}}^{(c)}[\vec{\theta}; q] = (E_c/T) \sum_{\mathbf{l}} (\nabla \cdot \vec{\theta}_{\mathbf{l}} - q)^2$. Alternatively one may shift the $\vec{\theta}$ field by $q\mathbf{l}$ to move the q -dependence into the pinning term $\frac{\gamma(T)}{2\pi^2} \cos(2\pi(\theta_i + ql_i))$. Since the grain coordinates l_i take integer values, the model is periodic in q -space with unit periodicity. Leaving the analysis of random background charges for future studies we will restrict ourselves to uniform gate voltages $q(\mathbf{l}) = q = \text{const.}$ throughout.

For small q , the system is in a particle-hole symmetric “neutral” state: as for $q = 0$, the ground state is given by $\vec{\theta}_{\mathbf{l}} = 0$. At some finite value $q = q^*$, a transition towards a charged (with a non-integer average number of electrons per dot) and spatially non-uniform ground state takes place. To find q^* , let us compute the soliton energy in the presence of q . Since the q -dependence of the Hamiltonian is a pure boundary effect, one immediately finds the soliton energy $T^*(q) = T^*(0) - 2qE_c$. At $q^* = T^*(0)/(2E_c)$ the soliton energy $T^*(q)$ vanishes. This marks the transition into the charged state: for $q > q^*$, solitons are created at no cost.

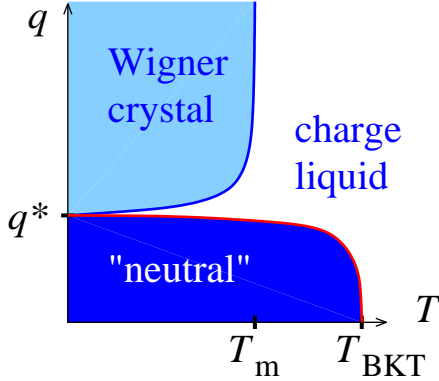


FIG. 8: (Color online) The phase diagram of the 2d array with a uniform background charge, q . In the “neutral” (insulating) phase, there are (almost) no solitons. Outside the neutral regime, charged solitons are generated. Below the melting temperature T_m , they form an insulating Wigner crystal.

It is instructive to relate the physics of the array to the phenomenon of vortex formation in type II superconducting films³⁶. Within this analogy¹¹, the gate voltage translates to an external magnetic field, H , and the gate voltage q^* corresponds to the critical magnetic field H_{c1} where vortex formation becomes energetically favorable.

Above H_{c1} a type II superconductor contains a finite density of vortices which at low enough temperatures form an Abrikosov lattice³⁹. In a clean film, the vortex lattice is free to move, but is easily pinned by the system boundaries, the underlying lattice structure

(as in Josephson junction arrays) or any sort of disorder^{37,38}. Upon increasing the temperature it will eventually melt^{16,40}, and above the melting temperature T_m most of the vortices are unbound. The melting temperature at finite $H > H_{c1}$ is smaller than the zero magnetic field Berezinskii–Kosterlitz–Thouless but parametrically of the same order⁴⁰. Thus, at $T < T_m$ the system is superconducting while at $T > T_m$ vortex motion leads to dissipation.

Translating back to our problem this means that at $q > q^*$ the solitons form a Wigner crystal once their density is sufficiently large such that the interaction is logarithmic. Only in the narrow interval $q^* < q < q^* + \xi_s^{-2}$ the system is in the conducting charge liquid state. Upon increasing the gate voltage, the Wigner crystal forms and, due to lattice pinning, the system is an insulator at temperatures smaller than the melting temperature. The latter is of the order of T_{BKT} . The phase diagram is shown in Fig. 8. Note that while for $q < q^*$ charge is carried by individual (thermally-activated) solitons, for $q > q^*$ the mobile charges are lattice defects, whose core energy is proportional to the logarithm of the lattice constant of the Wigner crystal.

E. DoS

As in the 1d case, interactions lead to a suppression of the tunneling DoS in the vicinity of the Fermi energy. Using Eq. (48), one finds that, in 2d, the suppression of the DoS is determined by the phase correlator

$$\begin{aligned} \sum_{\mathbf{q}} \langle |\phi_{\mathbf{q}}(\tau) - \phi_{\mathbf{q}}(0)|^2 \rangle &= 4T \sum_{\mathbf{q}, m} \frac{1 - \cos \omega_m \tau}{|\omega_m| (\frac{q}{\pi} \mathbf{q}^2 + \frac{|\omega_m|}{E_c})} \\ &= \frac{1}{2\pi g} \ln^2(gE_c \tau). \end{aligned} \quad (60)$$

The final expression for the DoS, thus, reads^{9,41}

$$\nu(\epsilon) \sim \nu_0 \exp \left[-\frac{1}{4\pi g} \ln^2 \frac{gE_c}{\epsilon} \right]. \quad (61)$$

As in one dimension, the suppression of the DoS becomes significant at a scale much larger than T^* , namely, at $\epsilon \sim gE_c e^{-2\sqrt{\pi}g}$. While this is a purely perturbative result, decreasing the energy further non-perturbative effects become important. Specifically, the finiteness of the soliton energy leads to a hard gap in the zero-temperature DoS,

$$\nu(\epsilon < T^*) \stackrel{T=0}{=} 0. \quad (62)$$

VI. CONCLUSIONS

We have studied transport properties of inelastic granular arrays. We find that charge quantization and the localization of a unit charge within a finite area play the

crucial role in the low-temperature behavior of these systems. This is the case even in systems where due to a large bare conductance $g \gg 1$ charge behaves like a fluid at high temperatures. At large g , the elementary charged excitations are solitons spreading over (exponentially) many grains. In contrast, for weakly coupled arrays ($g \ll 1$) charge is quantized on a single grain. The excitation energy of the solitons, T^* , determines the activation gap for the low-temperature conductivity. In 2d arrays, logarithmic interactions between solitons lead to a sharp BKT crossover to the high-temperature regime at a temperature T_{BKT} which is parametrically smaller than the activation gap: $T_{\text{BKT}} = T_{(2d)}^*/g \ll T_{(2d)}^*$. The most straightforward way to access this physics is to study the elementary excitations of the classical, dissipative charge model. The latter may be viewed as the low-frequency limit of the phenomenological charge model, Eq. (10), introduced in the context of a single dot^{20,21}. The reduction to the low-frequency (classical) sector proceeds through integrating out all the modes with frequencies higher than a certain bandwidth (eventually to be understood as the temperature.) This process renormalizes the initial amplitude of the cosine-potential $E_c e^{-\mathcal{G}_0/2}$, bringing it down to $E_c e^{-\mathcal{G}_0/2} (T/E_c)^{1-1/d}$. (The renormalization is due to the massless rotational modes, which rotate charge without compressing it. Such modes are absent in 1d, thus there is no renormalization for $d = 1$.) The effective bandwidth reaches the amplitude of the cosine-potential at a certain energy scale (freezing temperature) T_0 . The latter is determined by the condition:

$$\mathcal{G}_0 - \frac{2}{d} \ln(E_c/T_0) = 0. \quad (63)$$

It is reasonable to assume (based on the exact solution of the single-dot model²¹) that the renormalization of the potential stops at this scale. The physical reason behind this saturation is freezing-out of the rotational modes due to mass generation (by the cosine itself.) It is very important, however, to realize that in 1d and 2d the soliton energy is *larger* than the freezing temperature: $T^* \gg T_0$. As a result, the insulating behavior is established independently of the validity of the freezing assumption (the latter simply allows one to describe the insulator at $T < T_0$.)

In this paper we have derived the above mentioned phenomenology starting from the complementary phase-model. The latter is directly deducible from the microscopic fermionic Hamiltonian. The mapping between the two approaches is achieved by summation over instanton configurations (plus Gaussian fluctuations) of the phase-model. Curiously, the non-Gaussian fluctuations of the phase field around the instantons become strong at the same temperature scale T_0 given by Eq. (63). As was already mentioned above, the insulating behavior in 1d and 2d sets in at the scale T^* , which is parametrically larger than T_0 given by Eq. (63). Thus, the instanton gas summation is fully justified. In 3d, $T_{(3d)}^* \approx T_0$, and therefore instantons and non-Gaussian fluctuations be-

come important at the very same temperature, complicating the theoretical treatment. Our approach allows one, thus, to follow the behavior of the (1d and 2d) system from the metallic phase at high temperatures down to the insulating phase at low temperatures.

However, this luxury comes at the price of several key simplifications of the model. (i) The array is assumed to be perfectly uniform, i.e., we choose grain capacitances, C , inter-grain couplings, g , and (most restrictively) background charges, q , to be identical for all the grains. (ii) We have assumed a continuous spectrum in each grain. Doing this we have disregarded all manifestations of quantum coherence, such as Anderson localization, elastic hopping through several grains, etc. As a result, our treatment misses the physics at energy scales associated with the single-particle level spacing, δ . Thus, it provides only transient temperature dependencies — and not the ultimate low-temperature conductivity.

In principle, (random) fluctuations of the parameters (C , g , q) may be incorporated in our treatment. They will directly translate into static fluctuations of the corresponding parameters of the charge model. If such fluctuations are smooth and long-range correlated, solitons will continue to be the elementary charged excitations of the model. The difference is that now the solitons move in the presence of a random pinning potential. The problem is reduced to the dissipative dynamics of a *classical* gas of interacting solitons and anti-solitons subject to pinning. In 2d the very same model is used to describe the motion of vortices in type II superconductors, see, e.g., Refs. [38,42]. In 1d the conductivity of the array is determined by rare fluctuations causing anomalously strong soliton pinning⁴³. Strong short-range disorder, however, may invalidate the soliton picture. It is not known whether arrays with short- and long-range disorder display the same low-temperature behavior.

Incorporating quantum coherence is yet a more difficult task. To proceed in this direction, one has to take into account the finite level spacing δ in each grain. The most natural model assumes a random chaotic spectrum in each grain with Wigner-Dyson spectral statistics, mutually uncorrelated between different grains. Such a model necessarily includes randomness, even if all the other parameters are assumed to be strictly deterministic. Technically, the chaotic spectrum of a grain is described by the non-linear σ -model matrix field Q_1 . Since our ultimate goal is to describe the interacting system, either replica⁴⁴ or Keldysh⁴⁵ variants of the latter should be considered. In this case the Q_1 -field is a matrix in replica (Keldysh) space as well as in energy space. One thus faces a theory of two coupled fields: Q_1 and ϕ_1 . The perturbative renormalization (RG) group treatment of such a theory is well documented in the literature^{44,46}. In the absence of electron-electron interaction (no fluctuations of ϕ_1), the electron states in a low-dimensional ($d = 1, 2$) array are localized. Accounting for even small fluctuations of ϕ_1 results in a finite phase coherence length. This length gets shorter at higher tem-

peratures, and, in the case^{13,47} of $d = 2$, becomes of the order of the period of the granular array at $T \sim g^2 \delta$. At higher temperatures, single-particle localization is not important. However, as has been shown in this paper, if $\delta \ll E_c \exp[-g]$, the conductivity of an array still may be strongly suppressed due to the formation of charge solitons. Those appear due to the ϕ -field configurations with non-zero winding numbers, W , or instantons. The latter are absent in the perturbative RG, making it inadequate for the quantitative description of the insulating phase. It is known from the single-dot model⁴⁸ that the ϕ -field instantons induce non-perturbative rotations of the Q -matrix fields. The full theory accounting for the single-particle localization effect and for the charge solitons, should therefore contain *combined* instantons of ϕ and Q degrees of freedom⁴⁹. The experience in a non-perturbative treatment of replica (or Keldysh) non-linear σ -models is relatively limited, but rapidly growing. We should mention recent successful treatment of the Wigner-Dyson spectral statistics^{50,51,52}. Even more encouraging is the recent realization that Anderson localization in certain one-dimensional systems may be treated exactly by summing up all stationary configurations of the Q -matrix field with non-zero winding numbers^{53,54}. These developments make us optimistic that a quantitative treatment of the insulating phase of disordered interacting electronic systems may be attained rather soon.

Acknowledgments

We are grateful to K. B. Efetov, M. Fogler and A. I. Larkin for valuable discussions. Work at the University of Minnesota was supported by the A.P. Sloan foundation and the NSF grant DMR04-05212 (AK) and by NSF grants DMR02-37296, and EIA02-10736 (LG). JSM was partially supported by a Feodor Lynen fellowship of the Humboldt Foundation as well as by the U.S. Department of Energy, Office of Science, under Contract No. W-31-109-ENG-38. Work at the University of Cologne was supported by Sonderforschungsbereich SFB/TR 12 of the Deutsche Forschungsgemeinschaft.

APPENDIX A: PHASE MODEL

1. Derivation of the AES action

We start from a prototypical model consisting of one dot (D) coupled to a lead (L). The system is described by electronic degrees of freedom and its action is given by

$$S[\psi] = \sum_{i=D,L} S_i[\psi] + S_t[\psi] + S_c[\psi],$$

where the non-interacting action S_D (S_L) of the dot (lead), a tunneling term S_t , and the charging action, S_c ,

are given by, respectively,

$$\begin{aligned} S_i[\psi] &= \int_0^\beta d\tau \bar{\psi}_i(\tau) (\partial_\tau - \mu + H_i) \psi_i(\tau), \\ S_t[\psi] &= \int_0^\beta d\tau \left(\bar{\psi}_D(\tau) \hat{T} \psi_L(\tau) + \text{h.c.} \right), \text{ and} \\ S_c[\psi] &= E_c \int_0^\beta d\tau (\hat{N}_D(\tau) - q)^2, \end{aligned}$$

and $\psi(\tau)$ is an imaginary-time fermionic (Grassmann) field. Further,

- H_D (H_L) is the Hamiltonian of the dot (lead). The notation $\bar{\psi}_i H_i \psi_i$ implies a sum over the internal Hilbert space, i.e., $\bar{\psi}_i H_i \psi_i = \int d\mathbf{x} \bar{\psi}_i(\mathbf{x}) H_i \psi_i(\mathbf{x})$.
- \hat{T} is the tunneling operator between the dot and the lead. Its real space representation is given by some matrix $T(\mathbf{x}, \mathbf{x}')$ whose detailed structure we need not specify.
- $E_c = e^2/(2C)$ is the charging energy, where C is the self-capacitance of the dot, and $\hat{N}_D = \int d\mathbf{x} \bar{\psi}_D(\mathbf{x}) \psi_D(\mathbf{x})$ the number operator of the dot.
- $q = V_g C/e$ is the background charge on the dot set by an external gate voltage V_g .

The decoupling of the interaction part of the action is effected by the introduction of a Hubbard-Stratonovich field $V(\tau)$ with the physical significance of a voltage:

$$e^{-S_D[\psi] - S_c[\psi]} \longrightarrow \int \mathcal{D}V e^{-S[V] - S_D[\psi, V]},$$

where

$$\begin{aligned} S_c[V] &= \frac{1}{4E_c} \int_0^\beta d\tau V^2(\tau) - iq \int_0^\beta V(\tau), \\ S_D[\psi, V] &= \int_0^\beta d\tau \bar{\psi}_D(\tau) (\partial_\tau - \mu + H_D + iV(\tau)) \psi_D(\tau). \end{aligned}$$

The field V can be removed from the dot action S_D by the gauge transformation

$$\psi_D(\tau) \rightarrow e^{i\phi(\tau)} \psi_D(\tau), \text{ where } \dot{\phi}(\tau) = V(\tau). \quad (\text{A1})$$

However, that transformation requires some caution. The fermionic fields obey anti-periodic boundary conditions $\psi_D(0) = -\psi_D(\beta)$. In order to preserve this property, the field ϕ has to fulfill the condition $\phi(\beta) - \phi(0) = 2\pi W$, where $W \in \mathbb{Z}$. Therefore, the static contribution $V_0 = \int d\tau V(\tau)$ can only be removed up to $\delta V_0 = V_0 - 2\pi TW$, where $W = [V_0/(2\pi T)]$ is the closest integer to $V_0/(2\pi T)$. However, in the limit of negligible level spacing $\delta \rightarrow 0$, fluctuations around $\delta V_0 = 0$ are suppressed.

The gauge transformation (A1) couples to the tunneling terms

$$S_t[\psi] \rightarrow S_t[\psi, \phi] = \int_0^\beta d\tau \left(\bar{\psi}_D(\tau) \hat{T} e^{i\phi(\tau)} \psi_L(\tau) + \text{h.c.} \right).$$

Since the action is quadratic, the fermionic fields can be easily integrated out to yield a description in terms of the phase field ϕ only. Performing the Gaussian integration over ψ we obtain

$$S_t[\phi] = -\text{tr} \ln \begin{pmatrix} G_D^{-1} & \hat{T} e^{i\phi} \\ \hat{T}^\dagger e^{-i\phi} & G_L^{-1} \end{pmatrix},$$

where the trace extends over all index spaces (time, position, $i = D, L$) and $G_i^{-1} = \partial_\tau - \mu + H_i$.

As a next step, we expand the 'tr ln' in tunneling amplitudes,

$$S_t[\phi] = \sum_k \frac{1}{2k} \text{tr} \left[\left(G_D \hat{T} e^{i\phi} G_L \hat{T}^\dagger e^{-i\phi} \right)^k \right]. \quad (\text{A2})$$

Finally, the trace over the Hilbert spaces of dot and lead, respectively, leads to

$$S_t[\phi] = -\frac{1}{8} \sum_k \kappa_k \text{tr} \left[\left(\Lambda e^{i\phi} \Lambda e^{-i\phi} \right)^k \right], \quad (\text{A3})$$

where $\kappa_k = -4 \frac{(-1)^k}{k} \sum_\alpha (\pi^2 \nu_D \nu_L |T_\alpha|^2)^k$, ν_D (ν_L) is the density of states of the dot (lead) and

$$\Lambda(\tau - \tau') = -\frac{i}{\sin(\pi T(\tau - \tau'))}. \quad (\text{A4})$$

(In the main text, Λ is given in Matsubara representation.) Adding to this the phase representation of the charging action, $S_c[\phi] = \int d\tau \dot{\phi}^2 / (4E_c) - iq(\phi(\beta) - \phi(0))$, we obtain the phase action of the system, $S = S_c + S_t$.

The straightforward generalization of this result to d -dimensional array geometries is given by Eqs. (3), (4).

2. Fluctuation determinant

In this appendix we provide details of the computation of the determinants resulting from the integration over fluctuations around instanton solutions. We will discuss the cases of isolated dots, one- and two-dimensional arrays in turn.

a. Single quantum dot

We begin by expanding the action (12) to second order in deviations, $\delta\phi$, from $\phi_W(\{z\})$. Since the instantons are saddle point configurations, there are no linear terms in this expansion:

$$\delta S_{\text{inst}} = g \langle \delta\phi | \hat{F} | \delta\phi \rangle, \quad (\text{A5})$$

where the operator \hat{F} is given by

$$\hat{F}(z) = \bullet \Lambda_W(z) \bullet \Lambda - \frac{1}{2} \bullet \bullet \Lambda_W(z) \Lambda - \frac{1}{2} \Lambda_W(z) \bullet \bullet \Lambda,$$

and $\Lambda_W(z) \equiv e^{i\phi_W(z)} \Lambda e^{-i\phi_W(z)}$. The dots indicate places for $\delta\phi(\tau)$ in the matrix products. In a more explicit notation,

$$2\hat{F}(\tau, \tau') = \Lambda_W^{\tau, \tau'} \Lambda^{\tau' - \tau} + \Lambda^{\tau - \tau'} \Lambda_W^{\tau', \tau} - \delta(\tau - \tau') \int d\tau_1 [\Lambda_W^{\tau, \tau_1} \Lambda^{\tau_1 - \tau} + \Lambda^{\tau - \tau_1} \Lambda_W^{\tau_1, \tau}].$$

For $z = 0$, the operator \hat{F} is diagonal in the Matsubara frequency basis. Its spectrum is given by

$$\lambda_m^{(W)} = \begin{cases} 0, & 1 \leq |m| \leq |W|, \\ |m| - |W|, & |W| < |m|. \end{cases}$$

For $z \neq 0$, the eigenbasis has a more complicated form, but the eigenvalues are independent of z . For $W = 1$, the basis reads

$$|\varphi_m(z)\rangle = \begin{cases} u^{m+1} \frac{1 - uz^*}{u - z} & m \leq -2, \\ \sqrt{1 - |z|^2} \frac{1}{u - z} & m = -1, \\ \sqrt{1 - |z|^2} \frac{u - z}{1 - uz^*} & m = 1, \\ u^{m-1} \frac{u - z}{1 - uz^*} & m \geq 2, \end{cases} \quad (\text{A6})$$

where $u = \exp[2\pi i T \tau]$. [$m = 0$ corresponds to a constant shift which is of no interest.] The quadratic action is thus given by

$$S_{\text{inst}} = \mathcal{G}_0 |W| - 2\pi i W q + g \sum_m \lambda_m^{(W)} |\delta\phi_m|^2, \quad (\text{A7})$$

where $\delta\phi(\tau) = \sum_m \delta\phi_m |\varphi_m(z)\rangle$.

Now we can evaluate the partition function taking into account all instanton configurations. The partition function Z is given by Eq. (15),

$$Z = Z_0 \sum_W \frac{Z_W}{Z_0} e^{2\pi i W q}, \quad (\text{A8})$$

where Z_0 is the partition function in the absence of instantons. The contribution to the partition function Z_W corresponding to a certain winding number W consists of all configurations with $s + W$ instantons and s anti-instantons^{28,30}, where $s \geq \max\{0, -W\}$. Here we neglect the weak interaction between (anti-)instantons (cf. main text.) Thus,

$$\frac{Z_W}{Z_0} = \sum_{s=\max\{0, -W\}}^\infty \frac{(2s + W)!}{(s + W)! s!} \frac{Z_{2s+W}}{Z_0} \int (dz) \mathcal{J}^{(2s+W)}(z),$$

where $\mathcal{J}^{(w)}(z)$ is the Jacobian of the transformation to the collective coordinate basis $\{|m\rangle\} \rightarrow \{z, |\varphi_{m>w}\rangle\}$,

$$\mathcal{J}^{(w)}(z) = \frac{1}{w!} \det^{(w)} \left\| \frac{1}{1 - z_a z_{a'}^*} \right\|.$$

Furthermore, Z_w is obtained by Gaussian integration over the massive fluctuations $\delta\phi$, namely

$$\frac{Z_w}{Z_0} = e^{-\mathcal{G}_0 w} \left(\frac{\prod_{m=1}^{\infty} g \lambda_m^{(0)}}{\prod_{m=2}^{\infty} g \lambda_m^{(1)}} \right)^w = \left(g e^{-\mathcal{G}_0} \prod_{m>1} \frac{m}{m-1} \right)^w.$$

Rewriting the product $\prod_m(\dots) = \exp[\sum_m \ln(\dots)]$, one finds that it is dominated by large $|m|$. Therefore, it is sufficient to keep only the first term in an expansion in $\frac{1}{|m|}$ — an upper cut-off is provided by the charging term in the action. Thus,

$$\frac{Z_w}{Z_0} \simeq \left(g^2 \frac{E_c}{T} e^{-\mathcal{G}_0} \right)^w. \quad (\text{A9})$$

Finally,

$$\int d^{2w} z \det^{(w)} \left\| \frac{1}{1 - z_a z_{a'}^*} \right\| \sim \pi^w \ln^w \frac{E_c}{T}. \quad (\text{A10})$$

Putting all the components back together yields

$$\frac{Z_W}{Z_0} = \sum_{s=0}^{\infty} \frac{1}{(s + |W|)! s!} \left(\pi g^2 \frac{E_c}{T} e^{-\mathcal{G}_0} \ln \frac{E_c}{T} \right)^{2s + |W|} \quad (\text{A11})$$

and, subsequently,

$$\begin{aligned} \frac{Z}{Z_0} &= \sum_W e^{2\pi i W q} I_{|W|} \left(2\pi g^2 \frac{E_c}{T} e^{-\mathcal{G}_0} \ln \frac{E_c}{T} \right) \\ &= \exp \left[2\pi g^2 \frac{E_c}{T} e^{-\mathcal{G}_0} \ln \frac{E_c}{T} \cos(2\pi q) \right], \end{aligned} \quad (\text{A12})$$

where $I_\nu(z)$ is a Bessel function. This is the result quoted in the main text.

b. Fluctuation determinant of the 1d array

It is relatively straightforward to generalize the analysis of the previous section to an array geometry. The main difference to the single dot case is that the fluctuation matrix $F = \{F_{kl}\}$ has additional spatial structure, where the indices k, l label the dots in the array. With the notation

$$\lambda_m^{(k)} = \begin{cases} |m| & |W_{k+1} - W_k| = 0, \\ |m| - 1 & |W_{k+1} - W_k| = 1, \end{cases} \quad (\text{A13})$$

where m is the Matsubara index, the fluctuation matrix F for the array takes the form

$$F_{kk} = \lambda^{(k-1)} + \lambda^{(k)}, \quad F_{kk+1} = F_{k+1k} = -\lambda^{(k)}, \quad (\text{A14})$$

and $F_{kl} = 0$ otherwise. Here, we have put the instanton parameter $z = 0$. (This simplification is justified because the dominant contribution to the fluctuation determinant comes from high frequency fluctuations which are not significantly affected by the value of z .)

It turns out to be convenient to rewrite $F = F_0 - \delta F$, where F_0 is the fluctuation matrix on the flat configuration without instantons, $F_0^{kl} = |m|(2\delta_{k,l} - \delta_{k-1,l} - \delta_{k+1,l})$. By contrast, δF has non-zero entries only at the edges of the plateau:

$$\delta F_{kl} = \sum_{\{s, s+1\} \in \partial A} \left(\delta_{k,l} (\delta_{k,s} + \delta_{k,s+1}) - \delta_{k,s} \delta_{l,s+1} - \delta_{k,s+1} \delta_{l,s} \right), \quad (\text{A15})$$

where ∂A is the boundary of the plateau, i.e., $\{s, s+1\} \in \partial A$ means that $|W_s - W_{s+1}| = 1$.

Thus the fluctuation term $\mathcal{F} = \det F / \det F_0$ can be represented as

$$\begin{aligned} \mathcal{F} &= \prod_m \exp \left[\text{tr} \ln (|m| \tilde{F}_0 - \delta F) - \text{tr} \ln (|m| \tilde{F}_0) \right] \\ &= \exp \left[\sum_m \text{tr} \ln \left(1 - \frac{1}{|m|} \tilde{F}_0^{-1} \delta F \right) \right], \end{aligned} \quad (\text{A16})$$

where $F_0 = |m| \tilde{F}_0$.

The Matsubara sum starts with $m = 2$, i.e., there is no infrared divergence. The important contribution comes from large $|m|$. It is therefore sufficient to keep only the first term in $\frac{1}{|m|}$, i.e.,

$$\mathcal{F} \simeq \exp \left[- \sum_m \frac{1}{|m|} \text{tr} \left[\tilde{F}_0^{-1} \delta F \right] \right]. \quad (\text{A17})$$

Inverting the matrix \tilde{F}_0 we find $(\tilde{F}_0^{-1})_{kl} = \min\{k, l\} - \frac{kl}{M+1}$ which leads to

$$\text{tr} \left[\tilde{F}_0^{-1} \delta F \right] = \frac{2M}{M+1} = \begin{cases} 1 & M = 1, \\ 2 & M \rightarrow \infty. \end{cases} \quad (\text{A18})$$

We finally note that the summation over m has to be cut off at large frequencies $m \sim E_c/gT$ where the charging energy $\sim E_c^{-1} \omega_m^2$ and the dissipation action $\sim g|\omega_m|$ become comparable. This leads to the estimate $\sum_m |m|^{-1} \sim \ln(gE_c/T)$. Substitution of this formula along with Eq. (A18) into Eq. (A17) leads to the result (32).

c. Fluctuation determinant of the 2d array

The two-dimensional fluctuation determinant may be obtained by straightforward generalization of our discussion of the previous section. Concentrate for simplicity on the infinite system, $M \rightarrow \infty$, we find that (the Fourier representation) of the fluctuation matrix on the flat background (no instantons) is given by $F_0 = |m| \tilde{F}_0$, where

$$\tilde{F}_0(\mathbf{p}) = 4 \left(\sin^2 \frac{p_x}{2} + \sin^2 \frac{p_y}{2} \right). \quad (\text{A19})$$

To account for the presence of instantons, we again need to evaluate the quantity $\text{tr} [\tilde{F}_0^{-1} \delta F]$. Since δF has non-vanishing entries only at the boundary of the island with $W = 1$, one finds

$$\text{tr} [\tilde{F}_0^{-1} \delta F] = \sum_{\{\mathbf{s}, \mathbf{s} + \mathbf{e}_i\} \in \partial A} \left((\tilde{F}_0^{-1})_{\mathbf{s}\mathbf{s}} + (\tilde{F}_0^{-1})_{\mathbf{s} + \mathbf{e}_i \mathbf{s} + \mathbf{e}_i} - (\tilde{F}_0^{-1})_{\mathbf{s}\mathbf{s} + \mathbf{e}_i} - (\tilde{F}_0^{-1})_{\mathbf{s} + \mathbf{e}_i \mathbf{s}} \right),$$

where $\{\mathbf{s}, \mathbf{s} + \mathbf{e}_i\} \in \partial A$ means that the link between sites \mathbf{s} and $\mathbf{s} + \mathbf{e}_i$ crosses the boundary of the island, i.e., $|W_{\mathbf{s}} - W_{\mathbf{s} + \mathbf{e}_i}| = 1$. Using Eq. (A19), one obtains

$$\begin{aligned} \text{tr} [\tilde{F}_0^{-1} \delta F] &= \sum_{\{\mathbf{s}, \mathbf{s} + \mathbf{e}_i\} \in \partial A} \sum_{\mathbf{p}} \frac{\sin^2 \frac{p_i}{2}}{\sin^2 \frac{p_x}{2} + \sin^2 \frac{p_y}{2}} \\ &= \sum_{\{\mathbf{s}, \mathbf{s} + \mathbf{e}_i\} \in \partial A} \frac{1}{2} = \frac{L}{2}, \end{aligned}$$

where L is a number of links along the circumference of the island. Using the approximations (A17) and $\sum_m |m|^{-1} \sim \ln(gE_C/T)$ (which apply regardless of dimensionality) we then find that the fluctuation determinant is given by Eq. (52).

3. Conductance

To compute the conductance, we couple the action to source terms A_X ($X = L, R$),

$$S_t \rightarrow \frac{1}{8} \sum_k \kappa_k \sum_{X=L,R} \text{tr} \left[\left(\Lambda e^{i(\phi \pm A_X)} \Lambda e^{-i(\phi \pm A_X)} \right)^k \right].$$

Physically, these terms represent the vector potential of an electric field coupled to the system. The Kubo conductance, G , may be computed by taking two-fold derivatives of the partition function with respect to A_X at $A_X = 0$:

$$G = -\frac{\pi}{2} \lim_{\omega \rightarrow 0} \frac{T}{\omega} \Im [Q(i\omega_m)]_{i\omega_m \rightarrow \omega^+}, \quad (\text{A20})$$

where

$$Q(i\omega_m) = \frac{1}{Z} \frac{\delta^2 Z}{\delta A_R(\omega_m) \delta A_L(-\omega_m)} \Big|_{A_R=A_L=0}. \quad (\text{A21})$$

Representing the partition function as a sum over winding number sectors, one finds

$$Q(i\omega_m) = \frac{1}{Z} \sum_W e^{2\pi i W q} \left\langle \frac{\delta S_W}{\delta A_R(\omega_m)} \frac{\delta S_W}{\delta A_L(-\omega_m)} \right\rangle.$$

Or, taking into account instantons and anti-instantons,

$$Q(i\omega_m) = \frac{1}{Z} \sum_W e^{2\pi i W q} \sum_{s=0}^{\infty} \frac{(2s + |W|)!}{(s + |W|)! s!} q_m^{(2s + |W|)}, \quad (\text{A22})$$

where

$$q_m^{(w)} = 4g^2 \mathcal{Z}_w \int d^2 w z \mathcal{J}^{(w)}(z) \left\langle |\langle \delta \phi | \hat{F}_w | m \rangle|^2 \right\rangle_{\delta \phi}. \quad (\text{A23})$$

Furthermore,

$$\begin{aligned} &\left\langle |\langle \delta \phi | \hat{F}_w | m \rangle|^2 \right\rangle_{\delta \phi} \\ &= \sum_{k, k'} \lambda_l \lambda_{k'} \langle m | \varphi_k(z) \rangle \langle \varphi_{k'}(z) | m \rangle \langle \delta \phi_k \delta \phi_{-k'} \rangle_{\delta \phi} \end{aligned}$$

and, according to the action Eq. (A7), $\langle \delta \phi_k \delta \phi_{-k'} \rangle = \mathcal{Z}_w \delta_{kk'} / (2g\lambda_k)$. Thus,

$$q_m^{(w)} = 2g \mathcal{Z}_w \int d^2 w z \mathcal{J}^{(w)}(z) \langle m | \hat{F}_w(z) | m \rangle.$$

For small m , one finds

$$\langle m | \hat{F}_w(z) | m \rangle \simeq m \left(1 + \sum_{j=1}^w \ln |z_j|^2 \right) + \mathcal{O}(m^2). \quad (\text{A24})$$

Finally, using that

$$\mathcal{J}^{(w)}(z) \simeq \frac{1}{w!} \prod_{j=1}^w \frac{1}{1 - |z_j|^2}, \quad (\text{A25})$$

we obtain

$$\begin{aligned} q_m^{(w)} &\simeq 2g \frac{m}{w!} \mathcal{Z}_w \int d^2 w z \left(1 + \sum_{j=1}^w \ln |z_j|^2 \right) \prod_{j=1}^w \frac{1}{1 - |z_j|^2} \\ &= 2g \frac{m}{w!} \mathcal{Z}_w \left(\pi \ln \frac{E_c}{T} \right)^w \left\{ 1 + A w \frac{1}{\pi \ln \frac{E_c}{T}} \right\}, \quad (\text{A26}) \end{aligned}$$

where $A = -\pi^3/6$.

Substituting these results into Eq. (A22) we obtain

$$\begin{aligned}
Q(i\omega_m) &= 2mg \frac{Z_0}{Z} \sum_W e^{2\pi i W q} \sum_{s=0}^{\infty} \frac{1}{(s+|W|)!s!} \left(g^2 \frac{E_c}{T} e^{-\mathcal{G}_0} \ln \frac{E_c}{T} \right)^{2s+|W|} \left\{ 1 + A(2s+|W|) \frac{1}{\ln \frac{E_c}{T}} \right\} \\
&= 2mg(1 + 2Ag^2 \frac{E_c}{T} e^{-\mathcal{G}_0} \cos(2\pi q)).
\end{aligned}$$

Recalling that $\omega_m = 2\pi mT$ and substituting in Eq. (A20), one finds Eq. (20) for the conductance.

4. Coulomb gas mapping

We briefly review the mapping (1d Coulomb gas) \leftrightarrow (1d discrete sine-Gordon model)⁵⁵. The action of the latter is given by

$$S[\theta] = \frac{E_c}{T} \int dx \left\{ (\partial\theta)^2 - 2ge^{-\mathcal{G}_0/2} \cos(2\pi\theta) \right\}, \quad (\text{A27})$$

where we have used specific expressions for the charge and the fugacity matching our model parameters (cf. Eqs. (33) and (35).)

Starting from the Coulomb gas representation, Eq. (31), we introduce the density variable $\rho(x) = \sum_i \sigma_i \delta(x - x_i)$. Using the equality $1 = \int D\rho \delta(\rho(x) - \sum_i \sigma_i \delta(x - x_i)) = \int D\tilde{\theta} D\rho \exp[i\tilde{\theta}(x)(\rho(x) - \sum_i \sigma_i \delta(x - x_i))]$, we may rewrite the interaction term of the Coulomb gas in terms of the new variables and subsequently integrate out ρ . This obtains a representation in terms of the Lagrange multiplier field $\tilde{\theta}$,

$$\begin{aligned}
&\prod_{i=1}^{2k} \int dx_i e^{\frac{\pi^2 T}{E_c} \sum_{j,j'=1}^{2k} |x_j - x_{j'}| \sigma_j \sigma_{j'}} \\
&= \int D\tilde{\theta} e^{-\frac{E_c}{4\pi^2 T} \int dx (\partial\tilde{\theta})^2} \left| \int dx e^{i\tilde{\theta}(x)} \right|^k \left| \int dx e^{-i\tilde{\theta}(x)} \right|^k.
\end{aligned}$$

Instead of imposing strict charge neutrality, one may assume that positive and negative charges fluctuate independently,

$$\begin{aligned}
&\sum_{k=1}^{\infty} \left(e^{-\mathcal{G}(T)/2} \right)^{2k} \frac{1}{(k!)^2} \left| \int dx e^{i\tilde{\theta}(x)} \right|^k \left| \int dx e^{-i\tilde{\theta}(x)} \right|^k \\
&\rightarrow \prod_{\sigma=\pm 1} \sum_{k=1}^{\infty} \frac{1}{k!} \left(e^{-\frac{\mathcal{G}(T)}{2}} \int dx e^{i\sigma\tilde{\theta}(x)} \right)^k. \quad (\text{A28})
\end{aligned}$$

Performing the k -summations and relabeling $\tilde{\theta} \rightarrow 2\pi\theta$, we obtain $Z = \int D\theta \exp(-S[\theta])$, where the action is given by (A27).

APPENDIX B: CHARGE MODEL

1. Multi-channel contacts

In this appendix we discuss the generalization of the classical model derived in the main text (Sec. IIB) to $N \geq 2$ channels. For every channel $\alpha = 1 \dots N$ of a multi-channel contact, a field $\theta_\alpha(\tau)$ is introduced. In order to clarify the following evaluation scheme, the reflection coefficients r are given indices specifying the direction, contact, and channel. For simplicity, we consider the case of zero gate voltage $q = 0$ throughout. The quadratic action of a d -dimensional array of M^d grains with N channels in each of the dM^d contacts is then given by

$$S_2 = \frac{1}{T} \sum_{l,m} \left\{ \pi |\omega_m| \sum_{\alpha} \tilde{\theta}_{l,\alpha}^2 + E_c \left(\sum_{\alpha} \nabla \cdot \tilde{\theta}_{l,\alpha} \right)^2 \right\}, \quad (\text{B1})$$

while the backscattering is described by

$$S_r = -\frac{E_c}{\pi} \sum_{l,\alpha} \sum_i r_{il\alpha} \int_0^\beta d\tau \cos(2\pi\theta_{i,l,\alpha}). \quad (\text{B2})$$

Here, it is assumed that the high-energy modes $E_c < |\omega_m| < D$ have already been integrated out. [At energies larger than E_c , all modes are decoupled and, thus, can be integrated out for each channel separately.]

Only the dM^d symmetric modes $\theta_1 = \sum_{\alpha} \theta_{1,\alpha}$ couple to external parameters, such as gate voltages. We thus need to find an effective action for θ_1 by integrating out the $dM^d(N-1)$ asymmetric modes. To this end let us change variables from $\theta_{1,\alpha}$ ($\alpha = 1 \dots N$) to θ_1 and $\tilde{\theta}_{1,\alpha} = \theta_{1,\alpha} - (\theta_1 - \sum_{\alpha' > \alpha} \theta_{1,\alpha'})/(\alpha+1)$ ($\alpha, \alpha' = 1 \dots N-1$). While the charging term renders the symmetric fields θ_1 massive, all the asymmetric fields $\tilde{\theta}_{1,\alpha}$ are massless. As a result, in the perturbation theory in powers of $r_{il\alpha}$, terms containing the massless fields $\theta_{1,\alpha}$ in the exponents (cosines) vanish. Rewriting the backscattering action in terms of the new fields, one can see that the lowest order non-vanishing terms are of the order $\prod_{\alpha=1}^N r_{il\alpha}$, where the product runs over *all* channels of a given contact:

$$Z_N \sim E_c^N \prod_{\alpha=1}^N r_{i1\alpha} \int d\tau_\alpha \cos \left(\frac{2\pi}{N} \sum_{\alpha} \theta_{i,1}(\tau_\alpha) \right) \prod_{\alpha=1}^N \left\langle \exp \left\{ 2\pi i \left(\tilde{\theta}_{i,1\alpha}(\tau_\alpha) - \frac{1}{\alpha} \left(\tilde{\theta}_{i,1,\alpha}(\tau_N) + \sum_{\alpha' < \alpha} \tilde{\theta}_{i,1,\alpha}(\tau_{\alpha'}) \right) \right) \right\} \right\rangle_{\tilde{\theta}_{1,\alpha}}.$$

Taking the averages $\langle \dots \rangle_{\tilde{\theta}_{1,\alpha}}$ with the actions

$$S_\alpha[\theta_{i,1,\alpha}] = \frac{1}{T} \sum_m \frac{\alpha+1}{\alpha} \pi |\omega_m| \tilde{\theta}_{i,1,\alpha}^2, \quad (\text{B3})$$

we obtain $E_c^{1-N} \prod_{\alpha=1}^N \prod_{\alpha' > \alpha} (\tau_\alpha - \tau_{\alpha'})^{-2/N}$ for the product of correlators $\prod_{\alpha} \langle \dots \rangle_{\tilde{\theta}_{1,\alpha}}$. The re-exponentiated action of $\tilde{\theta}_1$ thus assumes the time non-local form

$$S[\vec{\theta}] = \sum_1 \left\{ \frac{1}{T} \sum_m \left(\frac{\pi}{N} |\omega_m| \tilde{\theta}_1^2 + E_c (\nabla \cdot \vec{\theta}_1)^2 \right) - \frac{E_c}{\pi} \sum_i \prod_{\alpha=1}^N r_{i1\alpha} \int d\tau_\alpha \prod_{\alpha' > \alpha} \frac{1}{(\tau_\alpha - \tau_{\alpha'})^{2/N}} \cos \left(\frac{2\pi}{N} \sum_{\alpha} \theta_{i,1}(\tau_\alpha) \right) \right\}. \quad (\text{B4})$$

As a next step, in analogy to the single-channel case (see Secs. IV B and V B), one may integrate out all the remaining modes except the static one, $\theta_{m=0}$. The prefactor of the cosine-term $E_c \prod_{\alpha=1}^N r_\alpha \equiv \frac{1}{2\pi} E_c \gamma_0$ is renormalized according to

$$\begin{aligned} \gamma_0 &\rightarrow \gamma(T) = \gamma_0 \exp \left\{ - \frac{2\pi^2}{N^2} \sum_{\alpha, \alpha'} \langle \theta(\tau_\alpha) \theta(\tau_{\alpha'}) \rangle_{\theta_{m \neq 0}} \right\} \\ &= \gamma_0 \exp \left\{ - \sum_{m \neq 0} f(\omega_m) \left(1 + \frac{2}{N} \sum_{\alpha, \alpha' > \alpha} \cos \omega_m \tau_{\alpha\alpha'} \right) \right\}, \end{aligned}$$

where

$$f(\omega_m) = 2 \frac{T}{(2M)^d} \sum_{\mathbf{q}} \left\{ \frac{\frac{1}{d}}{N E_{\mathbf{q}} + \pi |\omega_m|} + \frac{1 - \frac{1}{d}}{\pi |\omega_m|} \right\} \quad (\text{B5})$$

and $E_{\mathbf{q}} = 4E_c \sum_i \sin^2(\pi q_i / (2M))$.

Since typical time differences $\tau_{\alpha\alpha'} = \tau_\alpha - \tau_{\alpha'}$ are of the order $1/T$ (the time integrals are dominated by the upper limit of integration), the cosine-term inside the exponent may be disregarded. Performing the Matsubara summation, one thus finds $\gamma(T) = \gamma_0 (T/E_c)^{1-1/d}$.

Evaluating the multiple time integrations in the prefactor of the cosine, one finds that the integral over the center-of-mass time $\tau = \sum_{\alpha} \tau_\alpha / N$ contributes a factor $1/T$, while the integration over $N-1$ independent time differences $\tau_\alpha - \tau$ yields a constant c_N multiplied by the logarithmic factor³² $\ln E_c/T$ (following simply from power counting.) The same logarithmic factor appears in the framework of the phase model as a result of zero-mode integration. We shall not keep this logarithm explicitly because all our evaluations of γ are done up to a numerical factor only. As a result of these approximations, we reproduce the classical model with $\gamma(T) \sim (T/E_c)^{1-1/d} \prod_{\alpha=1}^N r_\alpha = (T/E_c)^{1-1/d} e^{-\mathcal{G}_0/2}$.

2. Classical dynamics of the charge model

Our strategy in dealing with the charge model was to eliminate all high-frequency degrees of freedom until only the zero Matsubara frequency remains. The resulting theory describes the classical statistical mechanics of interacting charges. This is perfectly sufficient to describe the thermodynamics of the system. To calculate the conductivity, however, one needs to retain the low-frequency ($\omega \ll T$) dynamics. The Matsubara formalism is not convenient for this purpose. Thus, we adopt the following strategy: we first switch to the Keldysh formulation and then integrate out the high-frequency components, reducing the theory to the classical, $\omega \ll T$, sector only.

For the sake of simplicity, we deal here with the 1d single-channel model, defined by Eq. (10). In the Keldysh formulation, the imaginary-time field $\theta(\tau)$ is substituted by the pair of *real-time* fields $\theta^{cl}(t)$ and $\theta^q(t)$, originating from the symmetric and antisymmetric combinations of the two branches of the Keldysh contour, respectively. The operator in the quadratic part of the action: $\pi |\omega_m| - E_c \nabla^2$ in Eq. (10) is transformed into a 2×2 matrix in $cl-q$ space. According to the general structure of the Keldysh technique³⁴, the $cl-cl$ element of this matrix must vanish (reflecting the fact that a field, purely symmetric on the two branches of the contour, has zero action.) The $cl-q$ and $q-cl$ elements are the retarded and advanced analytical continuations of the Matsubara operator: $\pm \pi i \omega - E_c \nabla^2 \rightarrow \pm \pi \partial_t - E_c \nabla^2$. Finally, the $q-q$ element is given by the fluctuation-dissipation theorem (in equilibrium): $2i\omega \coth(\omega/2T)$. In the classical limit, $\omega \ll T$, it reduces to $4iT$.

Integration over the high-frequency components of the fields leads to a renormalization of the backscattering amplitude, in exactly the same way as in Matsubara theory. The remaining renormalized backscattering part of the action, $\cos(2\pi\theta)$, transforms to $\cos(2\pi(\theta^{cl} + \theta^q)) -$

$\cos(2\pi(\theta^{cl} - \theta^q)) \approx -4\pi\theta^q \sin(2\pi\theta^{cl}) + O((\theta^q)^3)$. Anticipating that the quantum component fluctuates only weakly in the classical limit, we omit higher order terms in this expansion. As a result, the low-frequency part of the Keldysh action takes the form

$$S = \int dt \sum_j \left[2\theta_j^q \left(\pi \partial_t \theta_j^{cl} - E_c \nabla^2 \theta_j^{cl} + \frac{E_c \gamma}{2\pi} \sin(2\pi\theta_j^{cl}) \right) + 4\pi i T (\theta_j^q)^2 \right]. \quad (\text{B6})$$

One can transform the last term in this action, employing a Hubbard–Stratonovich transformation to the partition function $Z = \int D\theta^{cl} D\theta^q \exp[iS]$, as

$$e^{-4\pi T \int dt (\theta_j^q)^2} = \int \mathcal{D}\xi e^{-\int dt \left\{ \frac{1}{4\pi T} \xi_j^2 - 2i\xi_j(t) \theta_j^q(t) \right\}}. \quad (\text{B7})$$

Substituting this expression into Eq. (B6), one notices that the resulting action depends on $\theta_j^q(t)$ only linearly. As a result, the integration over this field leads to a func-

tional δ -function, imposing the following identity at every instance of time:

$$\pi \partial_t \theta_j^{cl} - E_c \nabla^2 \theta_j^{cl} + \frac{E_c \gamma}{2\pi} \sin(2\pi\theta_j^{cl}) - \xi_j(t) = 0. \quad (\text{B8})$$

This is the Langevin equation, where $\xi_j(t)$ is the noise with the correlator that may be read out from Eq. (B7), namely $\langle \xi_j(t) \xi_{j'}(t') \rangle = 2\pi T \delta_{jj'} \delta(t - t')$.

Finally, in the multi-channel case one must renormalize the backscattering amplitude γ , as discussed in appendix B 1 above. In addition, the coefficient in front of the time derivative must read π/g . This may be shown phenomenologically by requiring that without backscattering Eq. (B8) describes the dynamics of the classical RC-circuit. From the bosonization perspective, this coefficient is given by π/N , where N is number of channels, simply because in the weak backscattering limit $g \approx N$. As a result, one recovers Eqs. (44) and (45), used in the main text.

-
- ¹ P.W. Anderson, Phys. Rev. **109**, 1492 (1958).
² P. Sheng, B. Abeles, and Y. Arie, Phys. Rev. Lett. **31**, 44 (1973).
³ J.E. Mooij, B.J. van Wees, L.J. Geerligs, M. Peters, R. Fazio, and G. Schön, Phys. Rev. Lett. **65**, 645 (1990).
⁴ A. Gerber, A. Milner, G. Deutscher, M. Karpovsky, and A. Gladkikh, Phys. Rev. Lett. **78**, 4277 (1997).
⁵ R. Parthasarathy, Xiao-Min Lin, K. Elteto, T.F. Rosenbaum, and H.M. Jaeger, Phys. Rev. Lett. **92**, 076801 (2004).
⁶ G. Schön, and A.D. Zaikin, Phys. Rep. **198**, 237 (1990).
⁷ D.S. Golubev and A.D. Zaikin, Phys. Lett. **A169**, 475 (1992); G. Goeppert and H. Grabert, Euro. Phys. J. B **16**, 687 (2000).
⁸ I.S. Beloborodov, K.B. Efetov, A. Altland, and F.W.J. Hekking, Phys. Rev. B **63**, 115109 (2001).
⁹ K.B. Efetov and A. Tschersich, Europhys. Lett. **59**, 114 (2002); Phys. Rev. B **67**, 174205 (2003).
¹⁰ A. Altland, L.I. Glazman, and A. Kamenev, Phys. Rev. Lett. **92**, 026801 (2004).
¹¹ J.S. Meyer, A. Kamenev, and L.I. Glazman, Phys. Rev. B **70**, 45310 (2004).
¹² I.S. Beloborodov, K.B. Efetov, A.V. Lopatin, and V.M. Vinokur, Phys. Rev. Lett. **91**, 246801 (2003).
¹³ I.S. Beloborodov, A.V. Lopatin, and V.M. Vinokur, Phys. Rev. B **70**, 205120 (2004); preprint cond-mat/0504148.
¹⁴ Y.L. Loh, V. Tripathi, and M. Turlakov, preprint cond-mat/0501749.
¹⁵ J. Zhang and B.I. Shklovskii, Phys. Rev. B **70**, 115317 (2004).
¹⁶ J.M. Kosterlitz and D.J. Thouless, J. Phys. C **6**, 1181 (1973).
¹⁷ V.L. Berezinskii, Zh. Eksp. Teor. Fiz. **59**, 907 (1970) [Sov. Phys. JETP **32**, 493 (1971)].
¹⁸ R. Fazio and G. Schön, Phys. Rev. B **43**, 5307 (1991).
¹⁹ V. Ambegaokar, U. Eckern, and G. Schön, Phys. Rev. Lett. **48**, 1745 (1982).
²⁰ K. Flensberg, Phys. Rev. B **48**, 11156 (1993).
²¹ K.A. Matveev, Phys. Rev. B **51**, 1743 (1995); A. Furusaki and K.A. Matveev, Phys. Rev. B **52**, 16676 (1995).
²² S.E. Korshunov, Pis'ma Zh. Eksp. Teor. Fiz. **45**, 342 (1987) [JETP Lett. **45**, 434 (1987)].
²³ Omission of the Gaussian fluctuations in early treatments of the instanton gas¹⁸ lead to the erroneous conclusion that there is a quantum metal-insulator transition at $g_c \approx 1$ in 2d.
²⁴ If all T_α are small, S_t can be simplified by retaining only $\kappa_1 \simeq g$, where g is the dimensionless (tunneling) conductance of the contacts. In this regime,

$$S_t[\phi] = \frac{gT^2}{4} \sum_{\langle 1,1' \rangle} \int d\tau d\tau' \frac{\sin^2(\frac{1}{2}(\phi_{11'}(\tau) - \phi_{11'}(\tau')))}{\sin^2(\pi T(\tau - \tau'))}.$$

²⁵ D.S. Golubev and A.D. Zaikin, Phys. Rev. Lett. **86**, 4887 (2001); preprint cond-mat/0402306.
²⁶ D.V. Averin and Yu.V. Nazarov, Phys. Rev. Lett. **65**, 2446 (1990).
²⁷ S.V. Panyukov and A.D. Zaikin, Phys. Rev. Lett. **67**, 3168 (1991).
²⁸ X. Wang and H. Grabert, Phys. Rev. B **53**, 12621 (1996).
²⁹ Yu.V. Nazarov, Phys. Rev. Lett. **82**, 1245 (1999).
³⁰ M.V. Feigel'man, A. Kamenev, A.I. Larkin, and M.A. Skvortsov, Phys. Rev. B **66**, 054502 (2002).
³¹ D.S. Golubev and A.D. Zaikin, JETP. Lett. **63**, 1007 (1996).
³² I.L. Aleiner, P.W. Brouwer, and L.I. Glazman, Phys. Rep. **358**, 309 (2002).
³³ P.M. Chaikin and T.C. Lubensky, *Principles of Condensed Matter Physics*, Cambridge University Press 1997.
³⁴ A. Kamenev, in *Nato Science Series II*, Vol. 72, eds. I.V. Lerner *et al.*, pp. 313-340, Kluwer Academic Publishers, Dordrecht, 2002; cond-mat/0412296.

- ³⁵ J.E. Mooij, in *Percolation, Localization, and Superconductivity*, NATO ASI Series B, Vol. 109, eds. A.M. Goldman and S.A. Wolf, pp. 325-370, Plenum Press, 1983.
- ³⁶ P.G. de Gennes, *Superconductivity of Metals and Alloys*, W.A. Benjamin, New York, 1966.
- ³⁷ A.I. Larkin and Yu.N. Ovchinnikov, *J. Low Temp. Phys.* **34**, 409 (1979).
- ³⁸ G. Blatter, M.V. Feigel'man, V.B. Geshkenbein, A.I. Larkin, and V.M. Vinokur, *Rev. Mod. Phys.* **66**, 1125 (1994).
- ³⁹ A.A. Abrikosov, *Zh. Eksp. Teor. Fiz.* **32**, 1442 (1957) [*Sov. Phys. JETP* **5**, 1174 (1957)].
- ⁴⁰ B.A. Huberman and S. Doniach, *Phys. Rev. Lett.* **43**, 950 (1979); D.S. Fisher, *Phys. Rev. B* **22**, 1190 (1980).
- ⁴¹ I.S. Beloborodov, A.V. Lopatin, G. Schwiete, and V.M. Vinokur, *Phys. Rev. B* **70**, 073404 (2004).
- ⁴² P. Chauve, T. Giamarchi, and P. Le Doussal, *Phys. Rev. B* **62**, 6241 (2000), and references therein.
- ⁴³ We are indebted to M. Fogler for the discussion of this point; see also M.M. Fogler, *Phys. Rev. Lett.* **88**, 186402 (2002), and references therein.
- ⁴⁴ A.M. Finkelstein, *Zeitschrift für Physik B*, **56**, 189 (1984).
- ⁴⁵ A. Kamenev and A. Andreev, *Phys. Rev. B* **60**, 2218 (1999).
- ⁴⁶ D. Belitz and T.R. Kirkpatrick, *Rev. Mod. Phys.* **66**, 261 (1994).
- ⁴⁷ Ya.M. Blanter, V.M. Vinokur, and L.I. Glazman, preprint cond-mat/0504309.
- ⁴⁸ A. Kamenev, *Phys. Rev. Lett.* **85**, 4160 (2000).
- ⁴⁹ A.V. Andreev and I.S. Beloborodov, *Phys. Rev. B* **69**, 081406(R) (2004).
- ⁵⁰ A. Kamenev and M. Mezard, *J. Phys. A* **32**, 4373 (1999); *Phys. Rev B* **60**, 3944 (1999).
- ⁵¹ A. Altland and A. Kamenev, *Phys. Rev. Lett.* **85**, 5615 (2000).
- ⁵² E. Kanzieper, *Phys. Rev. Lett.* **89**, 250201 (2002).
- ⁵³ A. Lamacraft, B.D. Simons, and M.R. Zirnbauer, *Phys. Rev. B* **70**, 075412 (2004).
- ⁵⁴ A. Altland, A. Kamenev, and C. Tian, preprint cond-mat/0505328.
- ⁵⁵ See, e.g., N. Nagaosa, *Quantum Field Theory in Condensed Matter Physics*, Springer 1999.